AD-A092 841 INSTITUTE FOR DEFENSE ANALYSES ARLINGTON VA F/G 18/8
A STUDY OF STRATOSPHERE-TO-TROPOSPHERE TRANSFER USING RADIOACTI--ETC(U)
FEB 80 E BAUER DOT-FA77WA-3965
UNCLASSIFIED IDA-P-1456 FAA/EE-80-06 NL

1 OF 1
AD A092 841

END
DATE FILMED
1-81
DTIC

LEVEL

Technical Report Documentation Page

1. Report No.	2. Government Accession No.	3. Recipient's Catalog No.
FAA-EE-80-06	AD-A092 841	

4. Title and Subtitle
A STUDY OF STRATOSPHERE-TO-TROPOSPHERE TRANSFER USING RADIOACTIVE TRACER DATA IN A ONE-DIMENSIONAL PARAMETERIZATION

5. Report Date
February 1980

6. Performing Organization Code

7. Author(s)
Ernest Bauer

8. Performing Organization Report No.
IDA Paper P-1456

9. Performing Organization Name and Address
Institute for Defense Analyses
400 Army-Navy Drive
Arlington, Virginia 22202

10. Work Unit No. (TRAIS)

11. Contract or Grant No.
DOT-FA77WA-3965

12. Sponsoring Agency Name and Address
Department of Transportation
Federal Aviation Administration
Office of Environment and Energy
Washington, D.C. 20591

13. Type of Report and Period Covered
Final

14. Sponsoring Agency Code

15. Supplementary Notes

16. Abstract

This paper reviews radioactive tracer data to determine effective stratosphere-to-troposphere transfer rates for a one-dimensional parameterization. The basic data used are the time-dependent global stratospheric burdens of ^{95}Zr following six Chinese thermonuclear explosions between 1967 and 1976, and also the falloff in burdens of ^{90}Sr and excess ^{14}C following the very large Soviet and U.S. test series of 1961 and 1962.

The results of the Chinese explosions demonstrate that transfer of material from stratosphere to troposphere is fast in winter but slow in the summer of initial injection. It is best modeled by a seasonally varying eddy diffusivity profile, showing "fast" transport (e.g., Dickinson-Chang, Danielsen) for a winter injection, and fast transport delayed to the next winter for a summer injection.

The cloud rise height for the 1961-1962 tests is not well known, and so two models for the yield-altitude curve are used, following Chang et al. (1979): a "high" (Foley-Ruderman) and a "low" (Seitz) model. The overall time variation in stratospheric burden of ^{90}Sr and in stratospheric and tropospheric burdens of ^{14}C can be simulated best by relatively fast falloff, i.e., by using a *low* injection height (Seitz) and *fast* transport (e.g., Dickinson-Chang). The difference in falloff rate of stratospheric burdens of ^{90}Sr and of ^{14}C is due principally to the recycling of ^{14}C (as CO_2) from the troposphere, with minor corrections due to sedimentation of the aerosols carrying ^{90}Sr and the difference in effective injection height of these two tracers. ^{90}Sr is a tracer of fission yield, so that it weights the smaller bombs with a low injection height more heavily than does ^{14}C, which is proportional to the total yield.

17. Key Words	18. Distribution Statement
rates, transfer, stratosphere, troposphere, radioactive isotopes, tracer studies	This document is available to the public through the National Technical Information Service, Springfield, Virginia 22161.

19. Security Classif. (of this report)	20. Security Classif. (of this page)	21. No. of Pages	22. Price
UNCLASSIFIED	UNCLASSIFIED	84	

Form DOT F 1700.7 (8-72) Reproduction of completed page authorized

ACKNOWLEDGMENTS

I should like to thank Mr. K. Telegadas (National Oceanic and Atmospheric Administration, Air Resources Laboratory) for many discussions on fallout data, Dr. A. S. Mason (University of Miami, Tritium Laboratory) for sending me material in advance of publication, Dr. J. Gardner (Naval Research Laboratory) for the numerics of the DIFFUS computer code, Mrs. K. Gardner (Institute for Defense Analyses) for her excellent programming, diagnostics, and write-up of the code, Dr. R. C. Oliver (Institute for Defense Analyses) for numerous discussions, and Dr. H. S. Johnston (University of California at Berkeley) as well as Messrs. Mason, Oliver, and Telegadas for their excellent, careful, and critical reviews of a draft version of this paper.

ABSTRACT

This paper reviews radioactive tracer data to determine effective stratosphere-to-troposphere transfer rates for a one-dimensional parameterization. The basic data used are the time-dependent global stratospheric burdens of ^{95}Zr following six Chinese thermonuclear explosions between 1967 and 1976, and also the falloff in burdens of ^{90}Sr and excess ^{14}C following the very large Soviet and U.S. test series of 1961 and 1962.

The results of the Chinese explosions demonstrate that transfer of material from stratosphere to troposphere is fast in winter but slow in the summer of initial injection. It is best modeled by a seasonally varying eddy diffusivity profile, showing "fast" transport (e.g., Dickinson-Chang, Danielsen) for a winter injection, and fast transport delayed to the next winter for a summer injection.

The cloud rise height for the 1961-1962 tests is not well known, and so two models for the yield-altitude curve are used, following Chang et al. (1979): a "high" (Foley-Ruderman) and a "low" (Seitz) model. The overall time variation in stratospheric burden of ^{90}Sr and in stratospheric and tropospheric burdens of ^{14}C can be simulated best by relatively fast falloff, i.e., by using a *low* injection height (Seitz) and *fast* transport (e.g., Dickinson-Chang). The difference in falloff rate of stratospheric burdens of ^{90}Sr and of ^{14}C is due principally to the recycling of ^{14}C (as CO_2) from the troposphere, with minor corrections due to sedimentation of the aerosols carrying ^{90}Sr and the difference in effective injection height of these two tracers: ^{90}Sr is a tracer of fission yield, so that it weights the smaller bombs with a low injection height more heavily than does ^{14}C, which is proportional to the total yield.

CONTENTS

FIGURES

TABLES

TABLES

SUMMARY

This paper reviews radioactive tracer data to determine effective stratosphere-to-troposphere transfer rates in a one-dimensional (1-D) parameterization. Atmospheric motions cannot be described adequately in a 1-D parameterization, but 1-D codes have been used extensively in estimating the environmental impact of atmospheric injectants such as oxides of nitrogen from SSTs and halocarbons. Thus it is appropriate to evaluate different 1-D transport coefficients (K-profiles), in particular their limitations.

The basic data used here are:

- The time-dependent global stratospheric burden of ^{95}Zr following six Chinese thermonuclear explosions detonated at Lop Nor (40°) between 1967 and 1976.
- The time-dependent global stratospheric burdens of ^{90}Sr and excess ^{14}C following the very large Soviet (polar) and U.S. (tropical) nuclear test series of 1961 and 1962.
- Ground-based measurements of HTO (T = ^{3}H) in the 1960s. There are also airborne observations of HTO from 1975 onward, but the data are still being reduced and thus are not included here.

Some discussion is also given of the change in altitude profiles of ^{90}Sr and ^{14}C following the Soviet and U.S. test series.

These tracers all have somewhat different characteristics (Table 1-1, p. 1-3). ^{95}Zr and ^{90}Sr are fission fragments, so their intensity is proportional to fission rather than total yield. They are lodged on aerosols which are subject to settling and are precipitation scavenged in the troposphere.

HTO is a gaseous tracer of fusion yield which is precipitation scavenged and behaves somewhat like water. Excess ^{14}C, which is produced by reaction of neutrons with atmospheric nitrogen, is a tracer of total yield. It is carried as $^{14}CO_2$, which is a good tracer for atmospheric CO_2. Thus its fate is of particular interest from a climatic standpoint. CO_2 is a gas which is only slightly scavenged by precipitation (unlike the other tracers) and is only lost slowly at the ground, but in contrast to the other tracers it is recycled from the troposphere back into the stratosphere.

First, the data from six Chinese thermonuclear explosions are analyzed. These explosions had very similar yields of 2-4 megatons (Mt) and thus, presumably, similar injection heights ($\sim$ 18 km), all at the same place (Lop Nor, 40°N, 90°E), which provides a reasonable if not ideal simulation for mid-latitude injections such as those due to stratospheric aircraft, whose flight path peaks near 50-55°N. There are good ^{95}Zr burden data from all six explosions. These data show rough consistency in their seasonal variation, with slow fallout in summer and rapid fallout in winter (Fig. 2-2, p. 2-6). There are also limited stratospheric HTO data from two of the six Chinese explosions. These data are still being reduced and are thus excluded here; a preliminary examination suggests that the HTO data are roughly consistent with the ^{95}Zr data.

For winter injections a "fast" K-profile (i.e., one giving rapid transport near the tropopause, such as DC (Dickinson-Chang) or KD (Danielsen) (Fig. 4-1, p. 4-2) gives better results than a "slow" K-profile, such as WT (Whitten and Turco or "Wofsy-Type"), HN (Hunten), or CH-LO (Crutzen-Howard/Low). For times of one to three years after a summer or fall injection it is best to use a "fast" profile with the injection delayed to the following winter, or possibly a "slow" K-profile, but this latter does not appear to be satisfactory during the initial summer/fall season because it predicts too much initial fallout.

In view of the potential importance of the seasonal variation in the removal of injectants from the stratosphere, this is discussed next, and both the Chinese ^{95}Zr and the earlier U.S. and USSR ^{90}Sr fallout are reviewed. For summer, fall, and winter injections (there are no data on springtime injections) there is evidence for a seasonal variation, with very little fallout until winter (i.e., up to 6 months following a summer injection), and then there is roughly a 4-month delay between the beginning of fallout from the stratosphere (January-February) and the peak in ^{90}Sr in rain at the ground, which occurs in May-June.

Next, the time variations in stratospheric burdens of ^{90}Sr and ^{14}C (as $^{14}CO_2$) following the 1961-1962 test series are analyzed. Figure 2-7 (p. 2-13) shows the changing stratospheric burdens of these tracers (and of HTO) and the corresponding tropospheric burden of excess $^{14}CO_2$. The stratospheric burden of ^{90}Sr decreases much faster than that of ^{14}C, with the difference maximizing some 2-4 years after injection. The tropospheric burden of ^{14}C, some of which comes from the injection of the 1950s, is large; by contrast, the tropospheric burden of ^{90}Sr is very small.

Before one can model the time dependence of atmospheric burdens of ^{14}C and ^{90}Sr, one must determine the effective injection height, because in the 1950s and 1960s there were a variety of injections at different latitudes (U.S. injections equatorial, Soviet injections mainly polar) and altitudes or yields. Two different models of cloud height as a function of yield, as used by Chang et al. (1979), are considered here. A review of data finds little evidence for the higher cloud-rise model.

Computer modeling of the change in stratospheric ^{90}Sr and excess ^{14}C burdens, using all the variations discussed here, gives the following results:

1. ^{90}Sr falls out faster than ^{14}C, principally because of its different behavior near and on the ground, although there are small contributions due to the sedimentation of ^{90}Sr and its lower effective injection height (it is a tracer of fission yield, while ^{14}C is a tracer of total yield: the biggest bombs, which go to the greatest heights, have a relatively small fission fraction, so that ^{90}Sr in 1961-1962 was injected 1-2 km lower, on the average, than ^{14}C).

2. The decline in burdens (stratospheric and tropospheric for ^{14}C, and stratospheric for ^{90}Sr) is best explained by assuming a low injection height (which is in accord with most available data) and fast transport (which agrees with the conclusion for the Chinese tests). See Fig. 6-2 (p. 6-4) for ^{90}Sr and Fig. 6-3 (pp. 6-7, 6-8) for $^{14}CO_2$.

3. There is no need to postulate excessively rapid fallout of ^{90}Sr, or a large reservoir for ^{14}C at high altitudes.

Johnston, Kattenhorn, and Whitten (1976) studied the change in altitude profile of ^{14}C between 1963 and 1964-1970 using a 1-D representation of the data, and found that a relatively slow transport profile (HN, i.e., Hunten) best fitted the data. The work of Johnston et al. has been reviewed carefully, since their conclusion differs from that of the present study, and the following conclusions are drawn:

1. The analysis of Johnston et al. uses boundary conditions which we believe to be inappropriate for ^{14}C, with a strong sink at the bottom (1 km) and another sink at the top (50 km).

2. Since no 1-D parameterization can be expected to match the full complexity of stratosphere-to-troposphere transfer, should one intercompare the altitude profiles of mixing ratio or of number density of tracer, or the total stratospheric/tropospheric burdens, and at what times after injection? Johnston et al. emphasize matching profiles of mixing ratio and of number density at relatively short intervals by re-initializing their computation (so that the effect of the boundary conditions and of interhemispheric transfer is minimized). By contrast, the present work emphasizes the total stratospheric burden at relatively long times after injection.

3. Explicitly, 2-4 years after an effective injection in January 1963, one can get the same stratospheric burden of ^{14}C either by using fast (DC) transport with what we believe to be the correct lower boundary condition or by using relatively slow (HN) transport with an excessively strong sink at the bottom (Fig. 6-5, p. 6-13).

In conclusion, the present analysis provides a consistent explanation of available data for the decay in stratospheric burdens of ^{95}Zr following Chinese explosions, and of ^{90}Sr and ^{14}C following U.S. and USSR tests. Of the various factors considered here, the following are found to be in agreement with the data:

1. Seasonal variation in initial fallout from Chinese tests, with little or no fallout following a summer or fall injection until the following winter season
2. Fast transport (i.e., DC or KD model, rather than WT) following the 1961-1962 tests, and following Chinese injections in winter
3. Low injection-height models

4. Generally accepted physics for the boundary conditions of different tracers, for the sedimentation of aerosols, and for the relative injection height of ^{90}Sr and ^{14}C.

However, no 1-D eddy diffusivity profile can describe the complexity of actual transport over all relevant time scales, and so the user is urged to be sure that the parameterization is appropriate to the problem at hand.

1. INTRODUCTION

In investigating the stratospheric pollution due to aircraft and other artificial sources, one key problem has to do with how long injectants remain in the stratosphere, since for chemically active injectants such as NO_x (= $NO+NO_2+...$), HO_x (= $OH+HO_2+H_2O_2$), and ClX (= $Cl+ClO+...$) this is one crucial factor in determining their effect on the overall stratospheric photochemistry. At present, much or most of the modeling used for making policy decisions on stratospheric pollution treats the motions one-dimensionally, because the one-dimensional (1-D) models can be run more quickly and used more economically in sensitivity studies than can more complex, higher dimensional models.

It is evidently important to validate the transport models used. They have generally been based on the observed profiles of molecules such as N_2O and CH_4, which have a steady ground-level source, a fairly long atmospheric lifetime, and a postulated photochemical loss mechanism in the upper stratosphere. By contrast, radioactive tracers due to thermonuclear explosions provide an instantaneous point injection, generally present no chemistry, and have a relatively simple loss mechanism by wet or dry deposition on the ground or in the ocean. (Note that radioactive ^{14}C is transformed rapidly into $^{14}CO_2$ and then follows this species.)

The principal source of data for all radioactive tracers comes from the U.S. Department of Energy "Airstream" flights and the preceding Defense Nuclear Agency "Stardust" flights, which for the past 25 years have operated several times per

year over a corridor near the west coast of America from 75°N to the equator (to 50°S through April 1974) at altitudes up to 19.2 km. These aircraft data have been supplemented by balloon flights, mainly near 30°N and 30°S.

Here I first examine the falloff with time of the stratospheric burden of ^{95}Zr due to six Chinese thermonuclear explosions between June 1967 and November 1976. The same technique is then applied to the stratospheric burdens of ^{90}Sr and ^{14}C due to the Soviet and U.S. test series of 1961-1962. The characteristics of the different tracers are given in Table 1-1, and those of the Chinese versus Soviet and U.S. series are given in Table 1-2. The Soviet series provided a very large source (in both space and time), at a period when there were extensive measurement networks operational on a worldwide basis. By contrast, the Chinese tests provided fairly reproducible point injections of 2-4 Mt yield at a time when only limited fallout measurements were made. Regarding the tracers, ^{90}Sr and ^{95}Zr are physically comparable tracers, precipitation-scavengeable fission fragments. ^{95}Zr has a short half-life, i.e., a high initial activity per unit mass but correspondingly a short available observation time ($\lesssim$ 1 year), while ^{90}Sr has a longer half-life, a lower initial activity per unit mass, and a correspondingly longer available observation time. The concentration of ^{14}C is proportional to total yield (Mt) of the bomb, that of T is proportional to fusion yield, and those of ^{90}Sr and ^{95}Zr are proportional to fission yield. ^{14}C is only slightly scavenged by precipitation; it is a gaseous tracer which is recycled from the troposphere (as $^{14}CO_2$) and thus provides quite different information than do the fission fragments or HTO. HTO is scavenged by precipitation and is also lost by vapor exchange, so that it is considered to be a tracer for water.

For an application to stratospheric aircraft flight, all the tracers have the advantage that they are stratospheric

TABLE 1-1. CHARACTERISTICS OF DIFFERENT TRACERS

Isotope	Excess ^{14}C	HTO	^{90}Sr	^{95}Zr
Half Life[a]	5730 years	12.26 years	28.1 years	65 days
Origin	$n+{}^{14}N \rightarrow {}^{14}C+p$	$n+{}^{6}Li \rightarrow T+{}^{4}He$	Fission fragment	Fission fragment
Tracer of	Total yield	Fusion yield	Fission only	Fission only
Source	U.S. and Soviet tests, 1950s to 1962	U.S. and Soviet tests	U.S. and Soviet tests	6 Chinese tests, 1967-1976
Period of Record	1956-1974	Surface data, 1962-71 Some aircraft data, 1975-79	1953-1974	1967-present
Specific Characteristics	Note b	Note c	Note d	Note e

[a]Source: *Handbook of Chemistry & Physics*, 57th edition, 1976-77.

[b]Exists in the atmosphere mainly as $^{14}CO_2$ gas, which, like ordinary CO_2, is long-lived and chemically unreactive in the atmosphere. Its principal loss mechanism is slow absorption in the ocean, with an e-folding time of 4.5 years (see Machta, 1973).

[c]H_2O isotope. Behaves somewhat but not completely like water.

[d]Extensive data in 1960s because of health hazard (replaces Ca in milk). Found on aerosols which rain out--size and sedimentation rate not really well known.

[e]Found on aerosols which sediment and rain out, presumably similar to ^{90}Sr. Because of its short half-life, produces a relatively large signal for a relatively small initial input, but falls off rapidly.

TABLE 1-2. SOME CHARACTERISTICS OF THE SEPARATE TEST SERIES AS SOURCES OF RADIOACTIVE TRACERS

Advantages	Disadvantages
a. Soviet and U.S. Tests of 1961 and 1962	
Very large yield (340 Mt total).	Background (~170 Mt from the 1950s). The effect of this is significant for ^{14}C but not for ^{90}Sr.
Extensive fallout network operational; data on ^{14}C and ^{90}Sr for a long time as function of latitude and altitude.	Distributed Source: 90% high latitude ($75^{o}N$) 10% tropical
Ground-based HTO data.	Altitude range of individual injections not well known.
b. 6 Chinese Tests (June 1967 through November 1976)	
Mid-latitude source ($40^{o}N$, $90^{o}E$).	Relatively low yield implies background due to intervening French tests is important in some cases.
Similar yields of individual bombs imply similar injection heights.	^{95}Zr data only good for short time ($\leq$ 1 year).
Variation over the year gives seasonal variation.	No adequate ^{14}C or ^{90}Sr data.
Some atmospheric HTO data from 1975 on.	More limited sampling network than in early 1960s.

point injections in approximately the correct altitude range (for SSTs), around 18 to 20 km; the Chinese mid-latitude injections provide the closest simulation of the latitudes of aircraft (approximately 50-55°N) and also provide seasonal variability, while the Soviet high-latitude injections provide a higher-altitude, high-latitude source and a measure of recycling from the lower atmosphere, i.e., longer time behavior than can be observed from the lower-yield Chinese explosions.

Table 1-3 amplifies this discussion by indicating what data are used and what information is gathered from a given set of data so as to be able to decide between different K-profiles, which represent the customary 1-D parameterization of dynamics. Section 2 reviews the data used, Section 3 treats the problem of cloud rise height, Section 4 discusses different K-profiles, and Section 5 indicates details of the 1-D diffusion model used here. Comparison between data and computations is made in Section 6, and conclusions are presented in Section 7.

It must be stressed that the atmosphere is not one-dimensional, and thus any 1-D parameterization is very limited. In particular:

- 1-D models and correspondingly K-profiles are interpreted in three distinct ways that are not always compatible:
  1. As representing atmospheric conditions near 30°N, or generally at mid-latitude
  2. As representing a hemispheric average
  3. As representing a global average for a Northern Hemisphere mid-latitude injection.
- It will be shown that no single K-profile can account for all aspects of available radioactive tracer data (e.g., burden and profile at all times after injection),

but nevertheless these limitations show deficiencies of the 1-D parameterization rather than evidence of a lack of physical understanding.

TABLE 1-3. DATA USED AND INFORMATION GATHERED

a. Data Used

a.1. ^{95}Zr 1967-78 stratospheric burden from Telegadas 1974, 1976, 1979b.

a.2. HTO 1963-71 ground level data, IAEA (see especially Krey and Krajewski 1970).

a.3. ^{90}Sr 1954-72 stratospheric burden; data from National Academy of Sciences 1975, p. 110; data verified from Friend et al. 1961, Feely and Troutman 1971, and Leifer and Toonkel 1978.

a.4. ^{14}C 1955-69 stratospheric burden; data from Telegadas 1971.

a.5. ^{90}Sr and ^{14}C altitude profile of Johnston et al. 1976.

b. Information Sought

b.1. Overall stratosphere-to-troposphere transport, including seasonal variability, from ^{95}Zr data (a.1).

b.2. Testing of K-profiles, from ^{90}Sr data (a.3).

b.3. Short-term variability between ^{14}C, HTO, and ^{90}Sr may tell us about sedimentation, effective injection height differences, and differences in boundary conditions.

c. Ultimate Results

c.1. Intercomparison of different K-profiles in stratosphere and perhaps also in troposphere.

c.2. Verification of the boundary conditions.

c.3. Some sketchy information on injection height of bombs.

2. DATA USED HERE

2.1. ^{95}Zr DATA

Telegadas (1974, 1976, 1979c,d) provides altitude-latitude profiles and also total stratospheric burdens of ^{95}Zr from 1967 to 1978. Fig. 2-1 shows the stratospheric burden of ^{95}Zr (decay-corrected to the date of release) for the six Chinese thermonuclear explosions that have been detonated in the atmosphere. By far the largest part of the burden lies in the Northern Hemisphere (see, e.g., Telegadas 1974, Figs. 47-49).

Table 2-1 lists some characteristics of the Chinese atmospheric thermonuclear explosions considered here. Note that there were also some French thermonuclear explosions which contributed to the ^{95}Zr burden, but these have been separated from the Chinese debris in Telegadas' analysis of the data. Table 2-2 lists the actual data that are used here.

From Fig. 2-1 one sees that the stratospheric burden remains constant after a summer or fall injection until the following January or February, when significant fallout of the debris begins. The actual date varies a little from year to year; Telegadas' estimates are listed in Table 2-3. To display this seasonal variability of the data, in Fig. 2-2 are shown the stratospheric burdens normalized [to the maximum burden injected (Table 2-1)] and plotted on a seasonally adjusted basis.

In this way all the data fall more or less on top of one another, showing a synthetic 1- to 2-year model of how ^{95}Zr, or presumably any radioactive aerosol, falls out of the stratosphere after a pulsed injection at mid-latitude ($40^{\circ}N$) and approximately 18 km altitude (Telegadas 1974, Figs. 44-45).

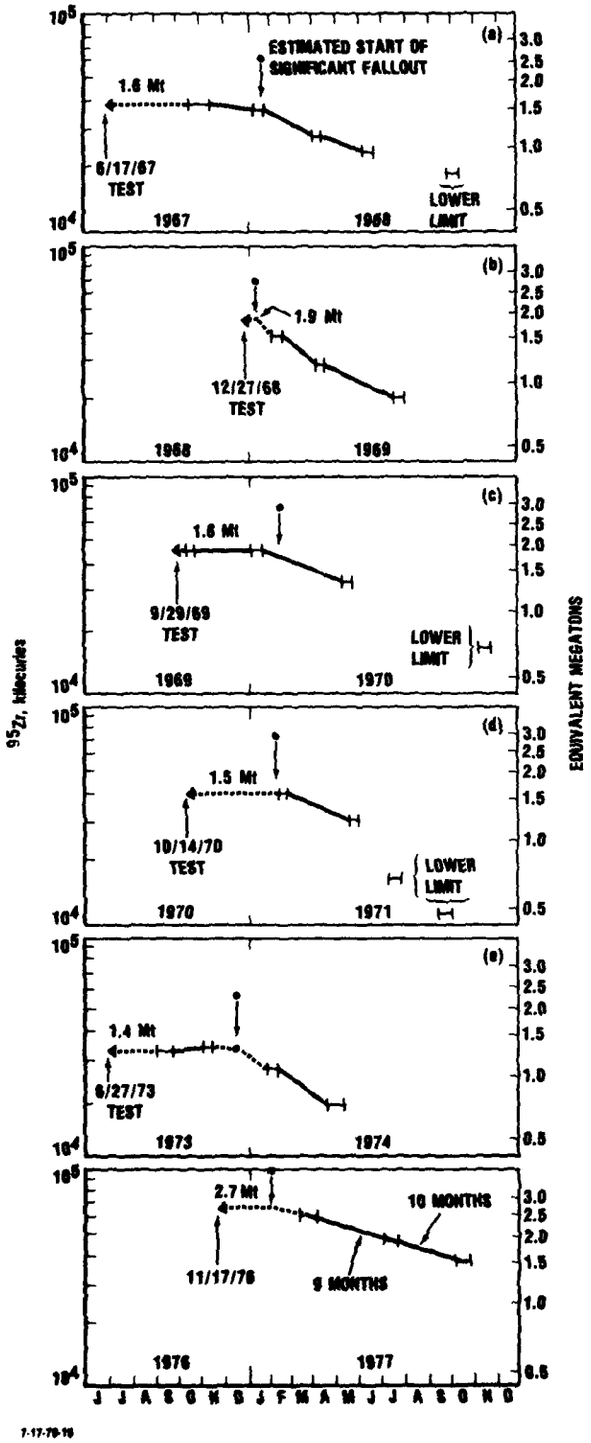

FIGURE 2-1. Stratospheric ^{95}Zr burden (decay corrected) following the Chinese nuclear tests. Observed burdens are indicated by the short horizontal lines. Note that, regardless of the date of injection, significant fallout from the stratosphere starts in the Northern Hemisphere winter season, demonstrating that stratosphere-to-troposphere transfer is much faster in winter than in summer of the injection hemisphere. (Source: Telegadas 1974, 1976, 1979b)

TABLE 2-1. LIST OF CHINESE ATMOSPHERIC THERMONUCLEAR EXPLOSIONS (ALL AT LOP NOR, 40°N, 90°E)

Date	Reported Yield,[a] Mt	Estimated Fission Yield,[b] Mt	Estimated Stratospheric Burden of ^{95}Zr,[c] MCi	Assumed Fusion Yield, Mt
17 Jun 1967	3	1.6	39	1.4
28 Dec 1968	3	1.9	46	1.1
29 Sep 1969	3	1.8	45	1.2
14 Oct 1970	3	1.5	38	1.5
27 Jun 1973	2.5 ("2-3")	1.4	35	1.1
17 Nov 1976	4	2.7	66	1.3

[a] DOE figures.

[b] Obtained from the estimated stratospheric burden of ^{95}Zr (Telegadas 1974, 1976, 1979c) by using the conversion factor 25.6 MCi ^{95}Zr/Mt fission (Harley et al. 1965).

[c] Telegadas 1974, 1976, 1979c.

TABLE 2-2. STRATOSPHERIC INVENTORY OF ZIRCONIUM-95 RESULTING FROM CHINESE TESTS

(Source: Telegadas 1974, 1976, 1979c,d)

Date	Predominantly Chinese Debris, kCi
17 June 1967 Test (decay-corrected to 17 June 1967)	
October 7 - November 9, 1967	38,500
January 8 - January 21, 1968	36,400
April 1 - April 7, 1968	27,200
May 30 - June 15, 1968	23,000
27 December 1968 Test (decay-corrected to 27 December 1968)	
February 3 - February 19, 1968	38,500
April 6 - April 9, 1969	27,800
July 14 - July 29, 1969	19,500
29 September 1969 Test (decay-corrected to 29 September 1969)	
October 13 - October 17, 1969	44,700
January 5 - January 20, 1970	45,300
May 6 - May 11, 1970	32,200
14 October 1970 Test (decay-corrected to 14 October 1970)	
February 22 - February 27, 1971	38,400
May 22 - May 28, 1971	29,800
27 June 1973 Test (decay-corrected to 27 June 1973)	
September 5 - September 19, 1973	33,200
October 30 - November 9, 1973	34,700
January 22 - February 2, 1974	28,300
April 12 - April 29, 1974	19,800
17 November 1976 Test (decay-corrected to 17 November 1976)	
March 22 - April 10, 1977	58,100
July 6-22, 1977	45,500
October 12-29, 1977	36,100
April 6-21, 1978	24,700

TABLE 2-3. ESTIMATED START OF SIGNIFICANT FALLOUT FOLLOWING CHINESE EXPLOSIONS

(Source: K. Telegadas, personal communication)

Code	Injection Date	Start of Fallout
M_1	17 Jun 67	15 Jan 68
M_2	27 Dec 68	15 Jan 69
M_3	29 Sep 69	15 Feb 70
M_4	14 Oct 70	15 Feb 71
M_5	27 Jun 73	15 Dec 73
M_6	17 Nov 76	1 Feb 77

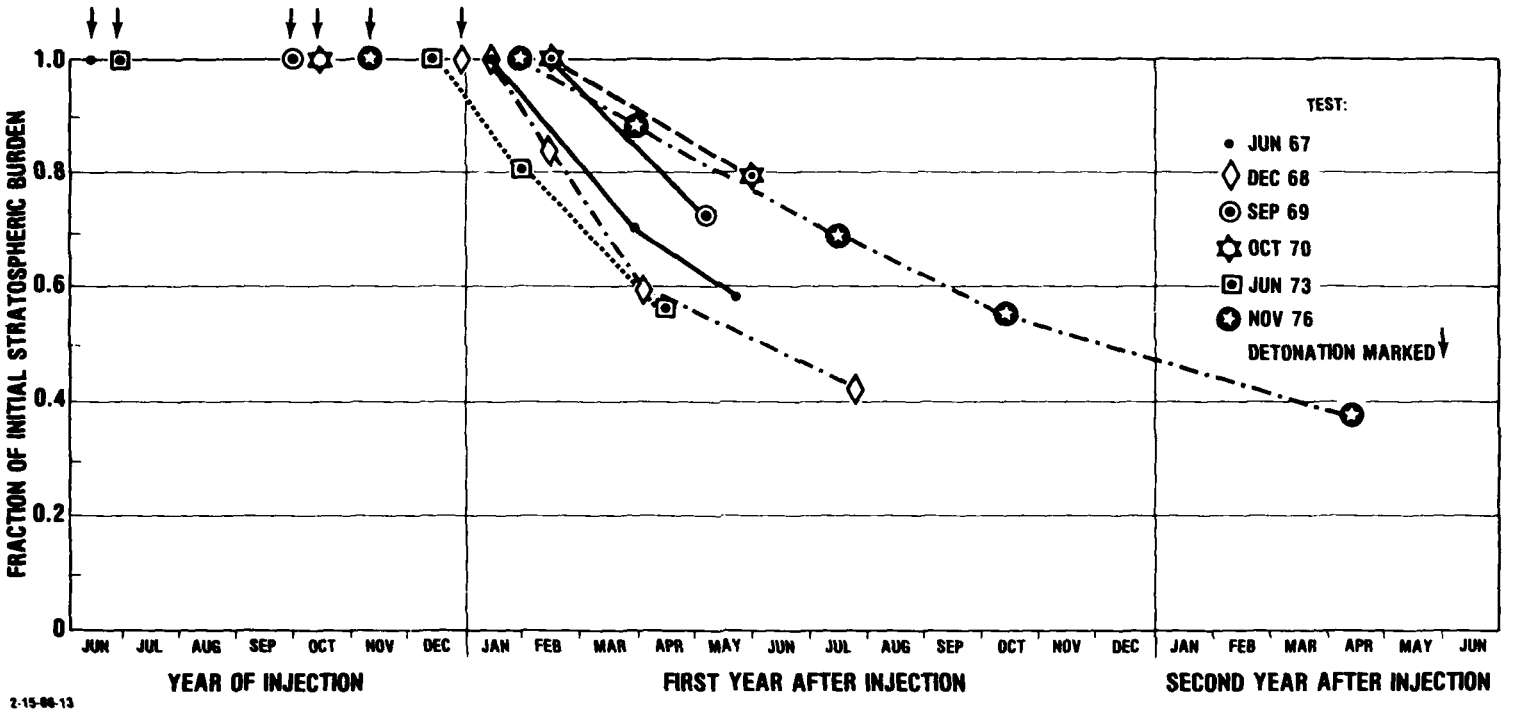

FIGURE 2-2. Composite seasonal depletion of stratospheric burden of ^{95}Zr (decay corrected to date of injection) for six Chinese thermonuclear explosions. Note that significant depletion only begins in the winter after the initial injection.

For comparison with Fig. 2-2, which demonstrates the seasonal character of fallout, Fig. 2-3 shows the same normalized burdens as a function of time after injection. I think it is reasonable to conclude, as did Telegadas, 1974, that seasonal variation is a significant factor in the fallout. Further, Fig. 2-4 plots the delay time T_1 between the injection (from Table 2-1) and the start of significant fallout (from Table 2-3). This again shows a definite relation between the month of injection and the time T_1 of initial fallout that is consistent with the observation that substantial fallout tends to begin in the spring following the initial injection.

The seasonal variations following the nuclear tests of the 1950s and 1961-1962 are discussed later (Section 2.5), but first I discuss HTO data following the Chinese explosions.

2.2. HTO DATA

During the 1960s there was an extensive network of ground-based stations for the collection of radioactive fallout. One tracer of interest here is tritium ($^3H = T$), which is a product of fusion. It is carried mainly as tritiated water, HTO, which can be a fairly good tracer for water vapor in the atmosphere.

HTO is normally considered to be precipitation scavenged in the troposphere, and thus the ground-based fallout is taken as a measure of loss from the stratosphere. Following the 1961-1962 tests there was evidence of a decline in stratospheric burden with a half-life of 16 months or an e-folding time of 23 months (Krey & Krajewski 1970; see also IAEA 1969, etc.).

Since 1975 airborne measurements of HTO and HT have been made a part of the Airstream program (Mason 1978). It had been hoped to analyze these data in the present work, but this has not been done because of delays in the resolution of some difficulties. A preliminary examination suggests that the HTO data are generally consistent with the ^{95}Zr results (personal communication, A. S. Mason & K. Telegadas).

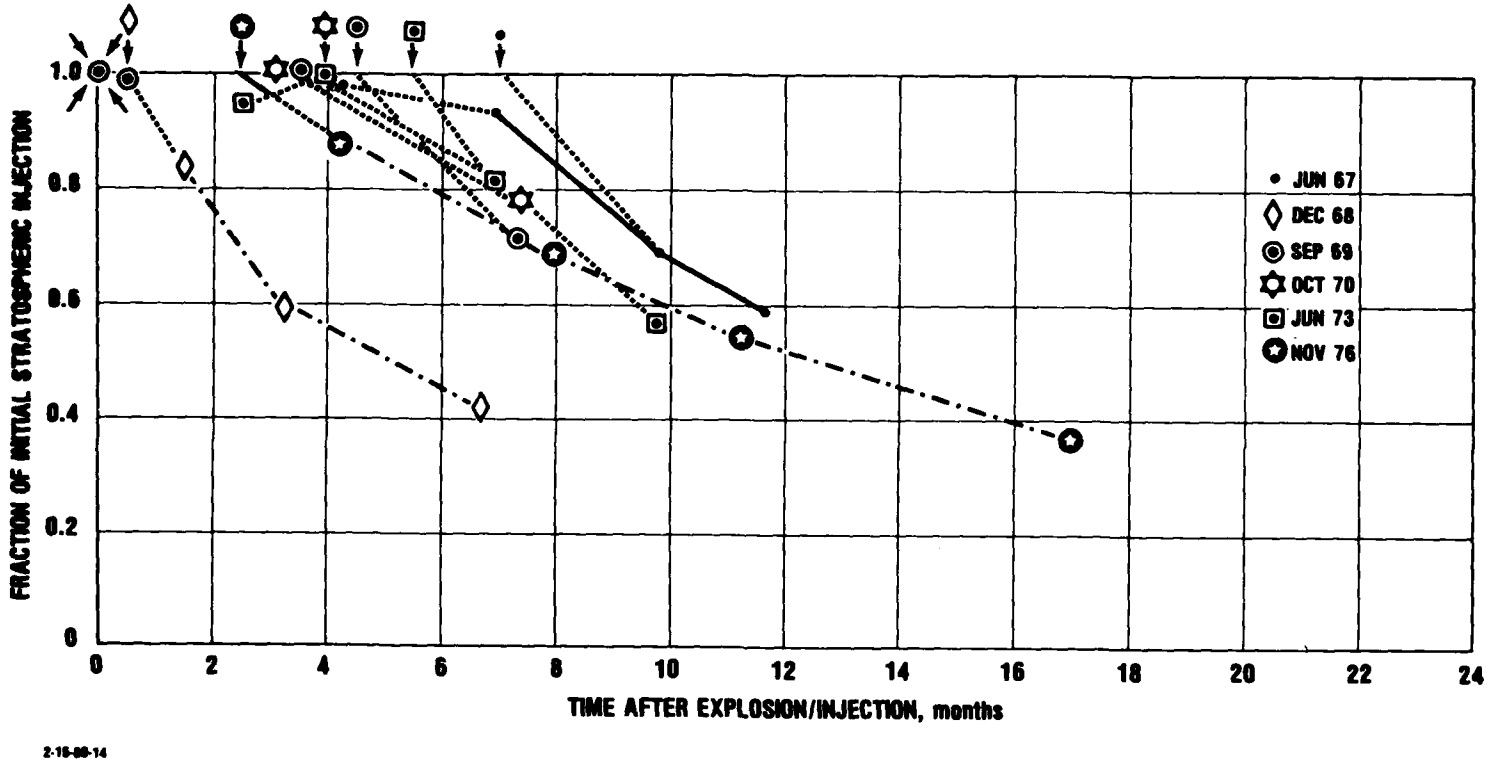

FIGURE 2-3. Depletion of normalized stratospheric burden of ^{95}Zr as a function of time after injection. Compare Fig. 2-2, which shows seasonal adjustment.

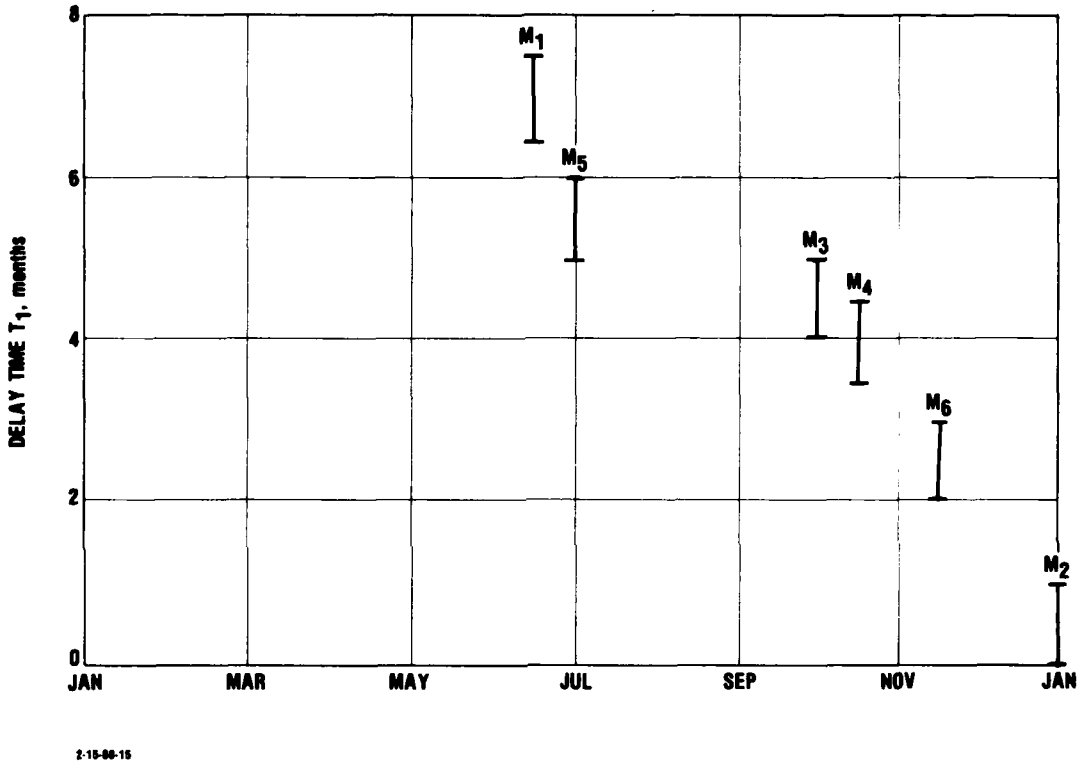

FIGURE 2-4. Delay time T_1 between date of injection (Table 2-1) and date of initial fallout (Table 2-3) for six Chinese thermonuclear explosions.

2.3. STRATOSPHERIC BURDENS OF ^{90}Sr AND ^{14}C DURING THE 1960s

Figure 2-5 shows the global stratospheric burden of ^{90}Sr for the period 1954-1972 (National Academy of Sciences 1975, p. 110, Fig. A.19; data verified from Friend et al. 1961, Feely & Trautman 1971, and Leifer & Toonkel 1978), and Fig. 2-6 shows the stratospheric burden of ^{14}C for the period 1955 to 1969 (National Academy of Sciences, op. cit., verified from Telegadas 1971). For a comparative analysis the stratospheric burdens of ^{14}C and ^{90}Sr are normalized to the same (maximum) value in January 1963, and they are plotted together in Fig. 2-7, which also shows the difference between the (normalized) stratospheric burdens of ^{90}Sr and ^{14}C and the tropospheric burden of ^{14}C (from Telegadas 1971). Figure 2-7 also shows the stratospheric burden of HTO inferred from ground-based data (Krey & Krajewski 1970).

Figure 2-7 will be used for comparison with different numerical models. A number of points should be made here:

- Table 2-4 shows the overall magnitude of the various atmospheric thermonuclear test series: the 1961-1962 test series provided the biggest input, but a significant background remained due to the testing of the later 1950s. One sees that the Chinese tests of 1967-1976 correspond to much smaller injections.
- Table 2-5 gives a detailed breakdown of the 1961-1962 test series, showing both fission and total yields; recall that ^{90}Sr production is proportional to fission yield, while ^{14}C production is due to total yield.
- On the scale of Fig. 2-7, where the peak injection corresponds to 340 Mt total or 96 Mt of fission, the peak injection due to a typical Chinese bomb, which has 1.5 Mt fission or 3 Mt total yield, would be $3/340 \simeq 0.01$ for ^{14}C, $1.5/244 \simeq 0.006$ for HTO, and

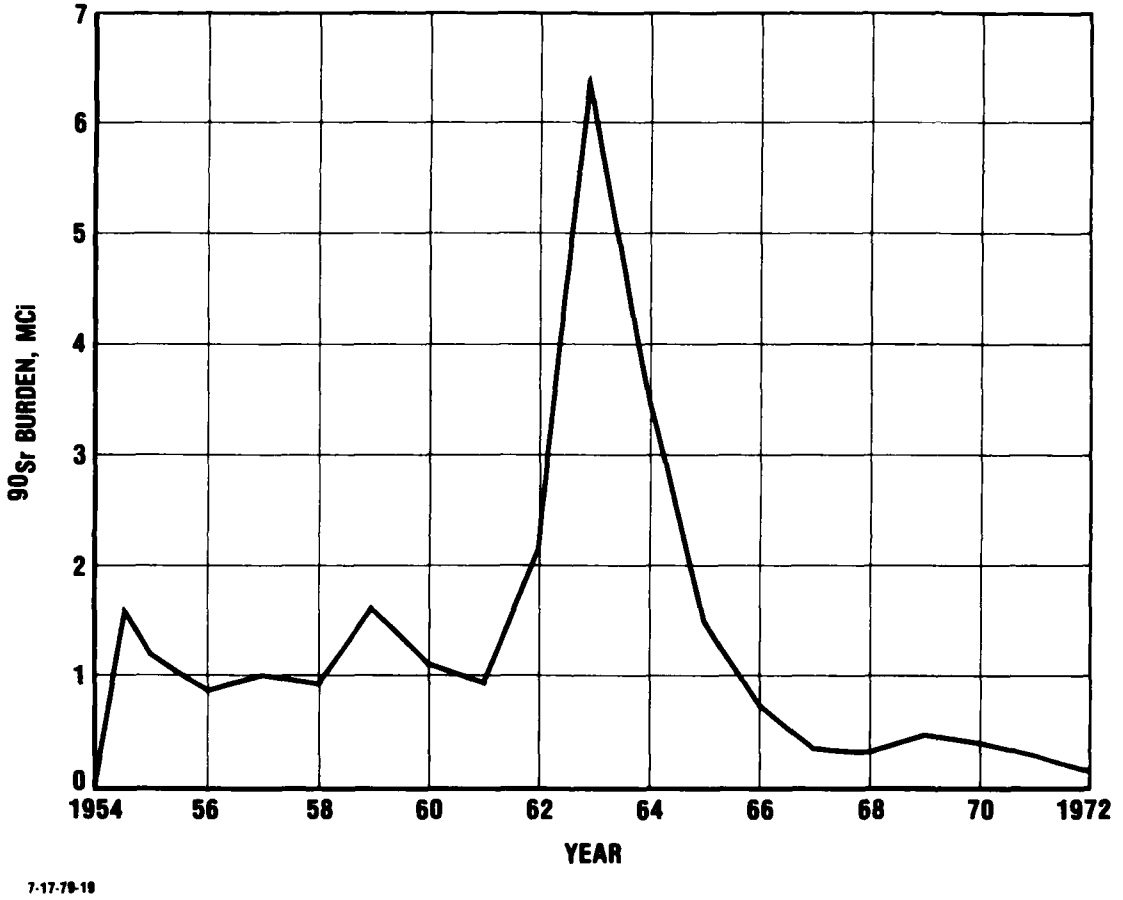

FIGURE 2-5. Global stratospheric burden of ^{90}Sr, 1954-1972. (Source: Table 1-3)

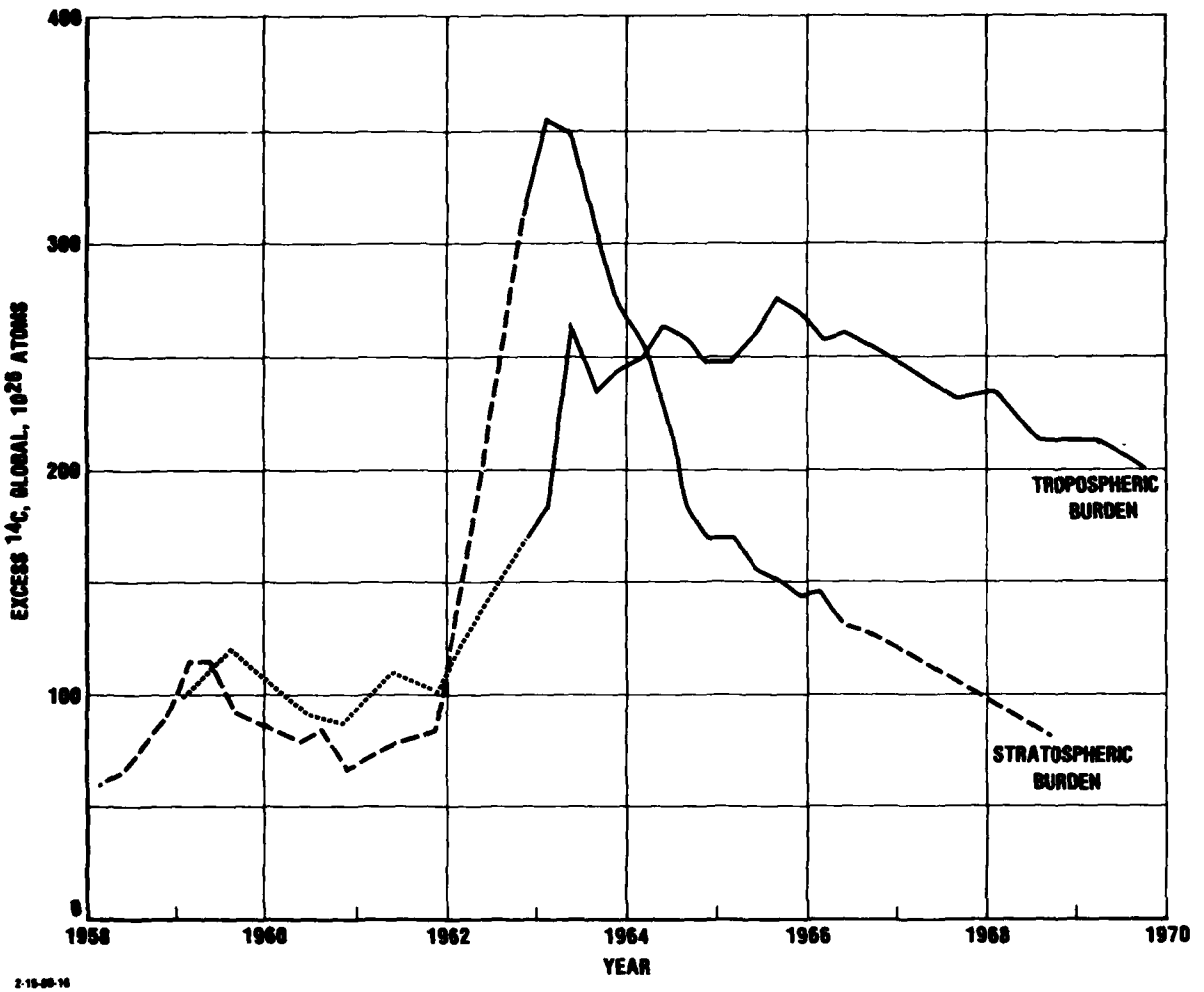

FIGURE 2-6. Global atmospheric burden of ^{14}C, 1955-1969. (Source: Table 1-3)

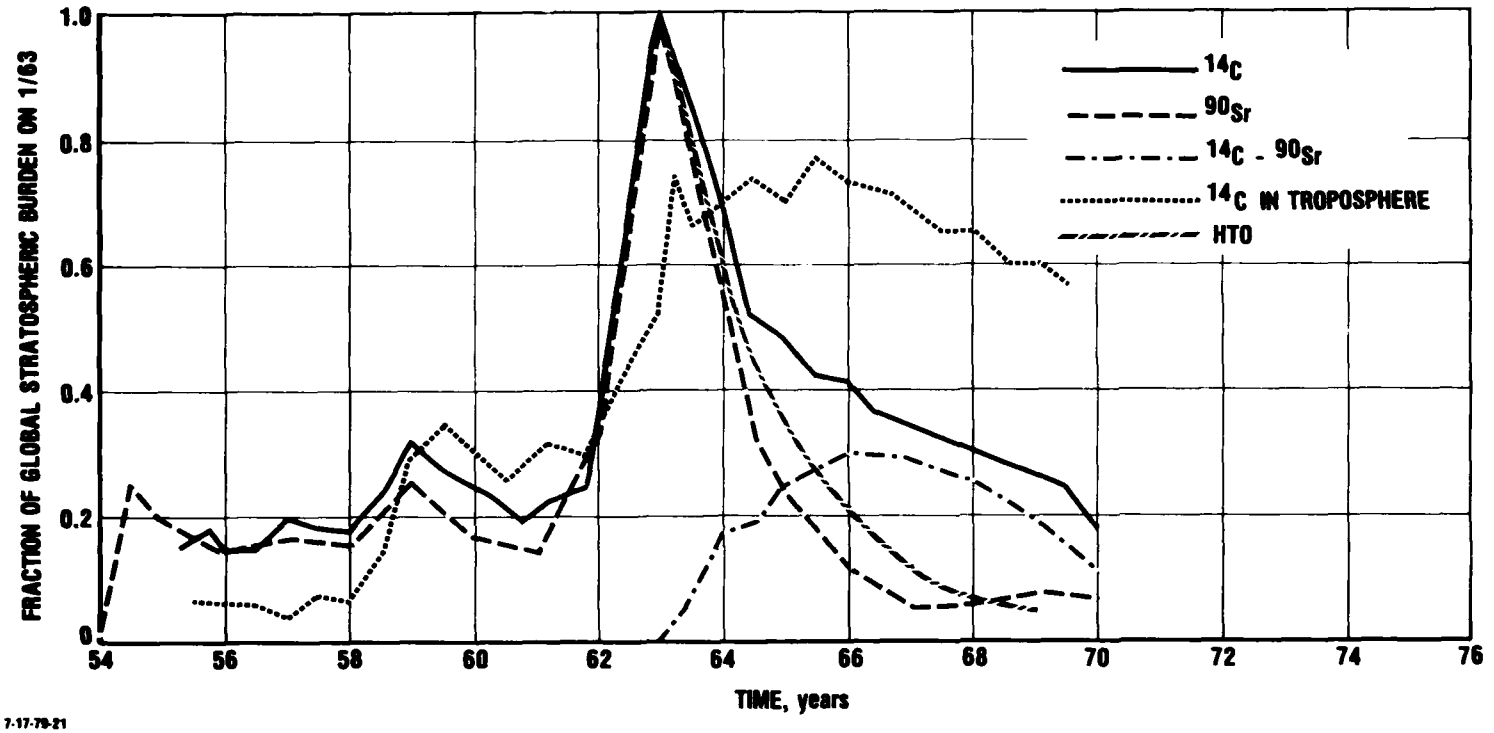

FIGURE 2-7. Normalized atmospheric burdens of ^{90}Sr, HTO, and ^{14}C. We show ^{14}C in the stratosphere and in the troposphere and ^{90}Sr and HTO in the stratosphere. (The tropospheric burden of ^{90}Sr would be very small because of rainout.) We also show the difference between stratospheric burdens of ^{14}C and ^{90}Sr, which has its maximum value in 1966, four years after the injection. The normalization used is the following: maximum stratospheric burden of ^{90}Sr = maximum stratospheric burden of HTO = maximum stratospheric burden of ^{14}C = 1 (all for January 1963). (Source: Table 1-3)

TABLE 2-4. CHRONOLOGY OF ATMOSPHERIC NUCLEAR TESTS

Time	Country/Location	Total Yield, Mt	
1952-54	U.S. (Tropical)	59	60
	USSR (Mid-high latitude)	1	
1955-56	U.S. (Tropical)	19	28
	USSR (Mid-high latitude)	9	
1957-58	U.S. (Tropical)	30	85
	U.K. (Tropical)	7	
	USSR (Mid-high latitude)	48	
1959-60	Moratorium: No atmospheric testing		0
1961	USSR (High latitude)	120	120
1962	U.S. (Tropical)	37	220
	USSR (High latitude)	180	
1963	Partial test ban treaty: No atmospheric testing		0
1967-68	France (Tropical)	4	10
	China (Mid-latitude)	6	
1969-70	France (Tropical)	2	8
	China (Mid-latitude)	6	
1971	France (Tropical)	1	1
1973	China (Mid-latitude)	2-3	2-3
1976	China (Mid-latitude)	4	4

TABLE 2-5. SUMMARY OF NUCLEAR TEST SERIES OF 1961 AND 1962

Country	No. of Detonations	Inclusive Dates	Latitude	Mean Date	Yield	
					Fission	Total
USSR	13	1 Sep - 4 Nov 61	52°N & 75°N	1 Oct 61	17	37
USSR	2	23 Oct (25 Mt) 30 Oct (58 Mt)	75°N	1 Nov 61	8	83
U.S.	7	25 Apr - 11 Jul 62	2°N & 17°N	1 Jul 62	11	37
		2 Oct - 4 Nov 62	17°N	15 Oct 62		
USSR	16	5 Aug - 24 Dec 62	52°N & 75°N	1 Oct 62	60	180

Source: Salter 1965, Table 1; Federal Rad. Council 1963, Tables 1-3.

1.5/96 ≃ 0.016 for ^{90}Sr or ^{95}Zr, which represent, respectively, total yield, fusion yield, and fission yield.

- Note that there appears to be a problem with the total ^{14}C budget (see Fig. 2-8) which suggests a larger input of ^{14}C than is observed with the global measurements. This may well be due to an uncertainty in the production rate or the number of ^{14}C atoms/Mt (see Machta et al. 1963).
- I shall only use the data following the 1961-1962 test series, but note the residual effects due to the earlier tests, which must be taken into account as providing a background.
- While the stratospheric burdens of ^{90}Sr and ^{14}C show general agreement, there are a number of differences:
  - The stratospheric ^{90}Sr burden falls off much more rapidly than does the ^{14}C burden.
  - Note the large ^{14}C burden in the troposphere; the tropospheric ^{90}Sr burden is very small.
- Note that the stratospheric HTO burden falls off almost as rapidly as that of ^{90}Sr and definitely faster than that of ^{14}C, especially at times in excess of 2.5 years.

2.4. SEASONAL VARIATION OF FALLOUT DURING THE 1950s AND 1960s

To supplement the discussion of seasonal variation in fallout from the Chinese tests (see Section 2.1, in particular Fig. 2-4), let us ask what can be learned from ^{90}Sr fallout data following the major thermonuclear tests of the 1950s and 1960s. A good data base for this is provided by HASL 1977, which is a tabulation of all available monthly fallout data of ^{90}Sr from 1954 through 1976. While there exist monthly

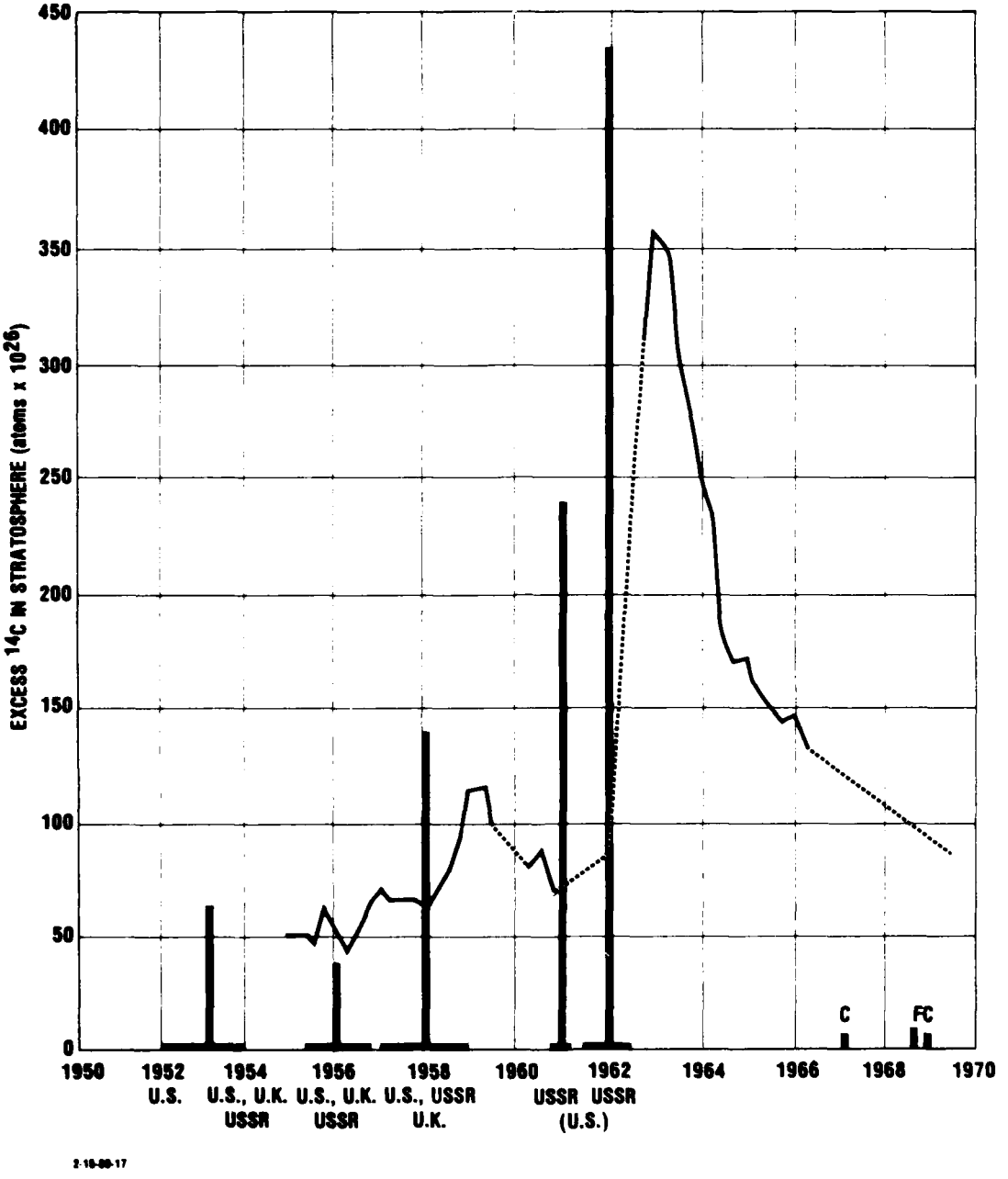

FIGURE 2-8. Excess stratospheric ^{14}C from atmospheric thermonuclear explosions. The total injected ^{14}C is shown [2 x 10^{26} atoms/Mt for airbursts, half that for surface bursts (Machta et al. 1963)] as well as the origin of the injection (U.S., U.K., F = tropical, USSR = arctic, C = mid-latitude). (Source of data: Telegadas et al. 1971)

global data from 1958 through the early 1970s and quarterly data thereafter (see, e.g., Volchok & Kleinman 1971, Feely 1976, Harley 1976). I shall use the monthly deposition data from New York City, which go from 1954 to the present, and which provide information comparable to that of Fig. 2-4 for the Chinese tests, with an indication (from the $^{89}Sr/^{90}Sr$ ratio) of how old the debris is.

The major stratospheric injections are listed in Table 2-6, with an indication (from HASL 1977, p. A-73ff.) of when (in what month) the peak in fallout occurred. The annual peak in fallout deposition (maximum monthly rate of fallout, MCi $^{90}Sr/km^2$) occurs generally between April and June, whereas the beginning of fallout from the stratosphere shown in Fig. 2-2 generally occurs in January-February. Thus there is a certain time delay, typically four months, between the beginning and the maximum of fallout.

In Fig. 2-9 are shown the time delay data from Table 2-6, including the data for the Chinese tests from Fig. 2-4, plotted as a function of the month of deposition. Each point is labeled with a letter for the latitude of injection [T = tropical, (i.e., U.S.), M = mid-latitude (i.e., China), P = polar (i.e., USSR)] together with a number (see Table 2-6) to characterize the specific injection. Points P3 and T4 correspond to injections over rather long time intervals and thus should not be given as much weight as the others. Nevertheless, it is clear that the data plotted in this way show a significant seasonal variation in fallout deposition, with the debris from injections at all latitudes being deposited in the spring.

Note also a current observation by Holloway, 1979, who finds that following the Chinese June 1973 injection the (decay-corrected) surface deposition of ^{91}Y and ^{144}Ce in July-October 1973 was 1% of that in March-June 1974.

TABLE 2-6. DELAY BETWEEN STRATOSPHERIC INJECTION AND FALLOUT

A. U.S. & Soviet Tests, 1956-1962[a]

Code No.	Country/Latitude	Yield, Mt/ No. Tests	Dates		Max. Surface Fallout Rate	Delay T_2, months
			Mean	Range		
T1	U.S./Tropical	10.5/5	6/56	5-7	4/57	10±1
P2	USSR/Mid-high	6/4	9/56	8-4	4/57	7^{+1}_{-2}
P3	USSR/Mid-high	12/5	6/57	4; 8-10	5/58	(11)
T4	U.S. & U.K./Tropical	21/30	6/58	11/57; 4-9	4/59	(10)
P5	USSR/Arctic	36/10	10/58	--	4/59	6
P6A	USSR/Arctic	37/13	10/61	9-11	2/62	4±1
P6B	USSR/Arctic	83/2	11/61	--	7/63	8
T7A	U.S./Tropical	37/7	7/62	4-7	7/63	12+3
T7B	U.S./Tropical		10/62	10-11	7/63	6-1
P8	USSR/Arctic	180/16	10/62	8-12	7/63	9±2

B. Chinese Tests (all at 40°N)

Code No.	Date	Initial Fallout[b]	Fallout Maximum[c]	Delay Times, months	
				to Initial Fallout (T_1)	to Fallout Maximum (T_2)
M1	6/67	15 Jan	5/68	7	11
M2	12/68	15 Jan	5/69	0.5	6
M3	9/69	15 Feb	6/70	4.5	9
M4	10/70	15 Feb	5/71	4.0	7
M5	6/73	15 Dec	5/74	5.5	11
M6	11/76	1 Feb	--[d]	2.5	--

[a] Injections: see, e.g., Bauer 1978, Table B-7, p.B-21ff.
Fallout: see HASL 1977.

[b] From Telegadas, personal communication.

[c] From HASL 1977.

[d] Only quarterly data.

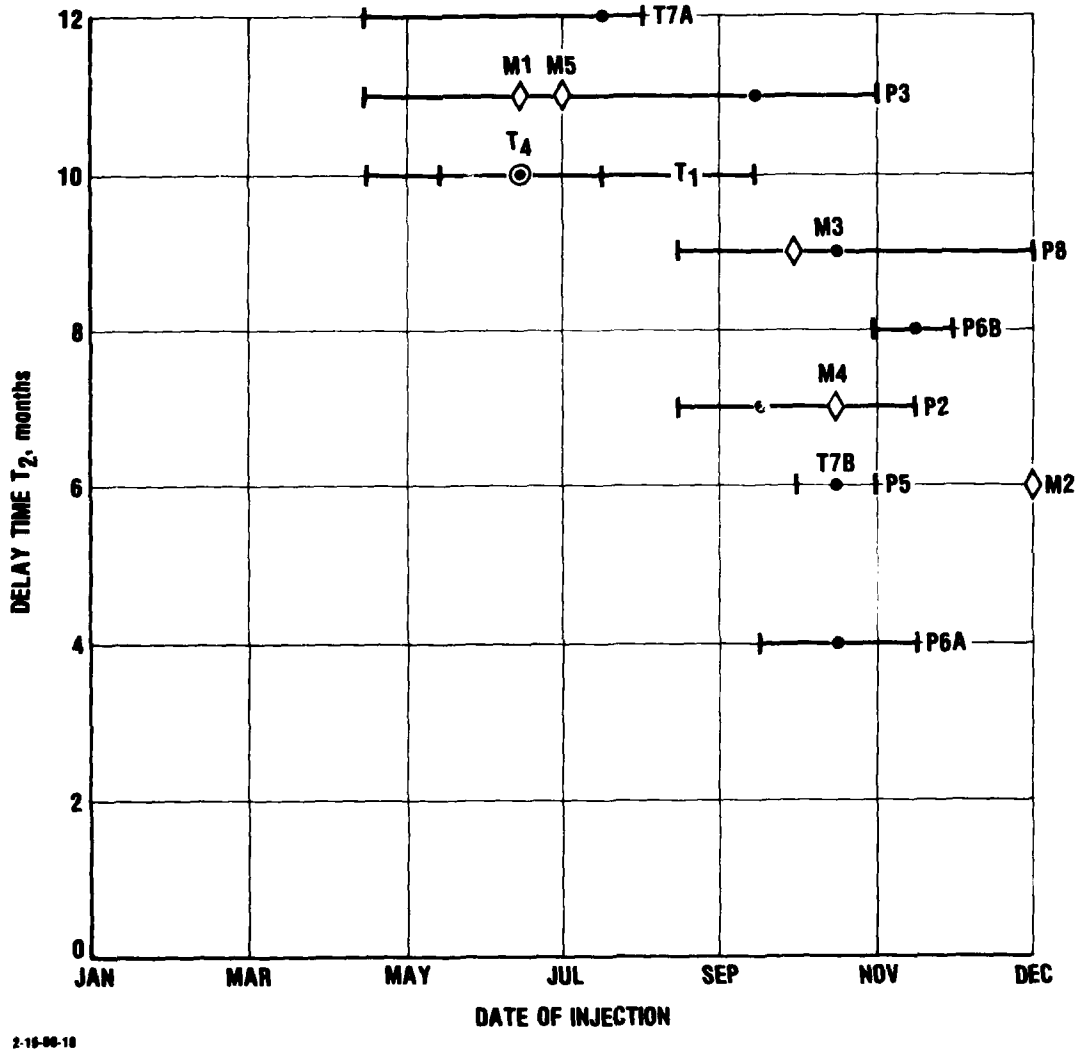

FIGURE 2-9. Delay time between stratospheric injection and maximum surface fallout rate. The points are identified in Table 2-6: T = tropical, M = mid-latitude, P = polar injection. This shows a seasonal variation in fallout.

Reference should be made to earlier discussions of NOAA (e.g., Machta 1965, Telegadas 1974) which point out that careful, long-term observers of fallout conclude that there is a seasonal variation in fallout. The present discussion supports this. Note, however, that there are anomalies in the annual fallout deposition cycle, in that fresh debris was observed shortly after the very large stratospheric injections of 1961 and 1962.

3. THE PROBLEM OF NUCLEAR CLOUD RISE AND DEBRIS INJECTION HEIGHT

During the 1961-1962 test series, some 38 thermonuclear devices with a total yield of approximately 340 Mt were fired, 10% in tropical and 90% in polar latitudes (Table 2-5). For modeling both the chemical and transport effects of such injections, one needs to know, or at least to hypothesize, how high the clouds went. One does know that weapons with yields greater than several megatons deposit most of their debris in the stratosphere and that the effective rise height increases with increasing yield.

Figure 3-1 shows several models of cloud rise height as a function of yield. The wide scatter indicates the variability and uncertainty of the results. Thus Peterson (1970) has constructed a model of cloud rise height based on U.S. data in the tropics and at the Nevada Test Site ($37^{\circ}N$) for low-yield tests. Peterson has extended his model to high-latitude (Soviet, $75^{\circ}N$) tests based on considerations of atmospheric stability. Note that the largest U.S. test was a 15-Mt surface burst (equivalent airburst yield 7.5 Mt), so beyond this yield there are no experimental data to support his model. Seitz et al. (1968) have established a model of cloud rise height for both the U.S. and USSR 1961-1962 test series as an input for testing the transport of various radioactive tracers and thus the observed profiles for ^{14}C, ^{90}Sr, and other tracers. See Figs. 3-2 and 3-3 for representative profiles. However, the cloud height models of Seitz et al. (1968) for the Soviet bombs shown in Fig. 3-1 are not the result of direct measurements. Telegadas' (1979b) model for Chinese (mid-latitude,

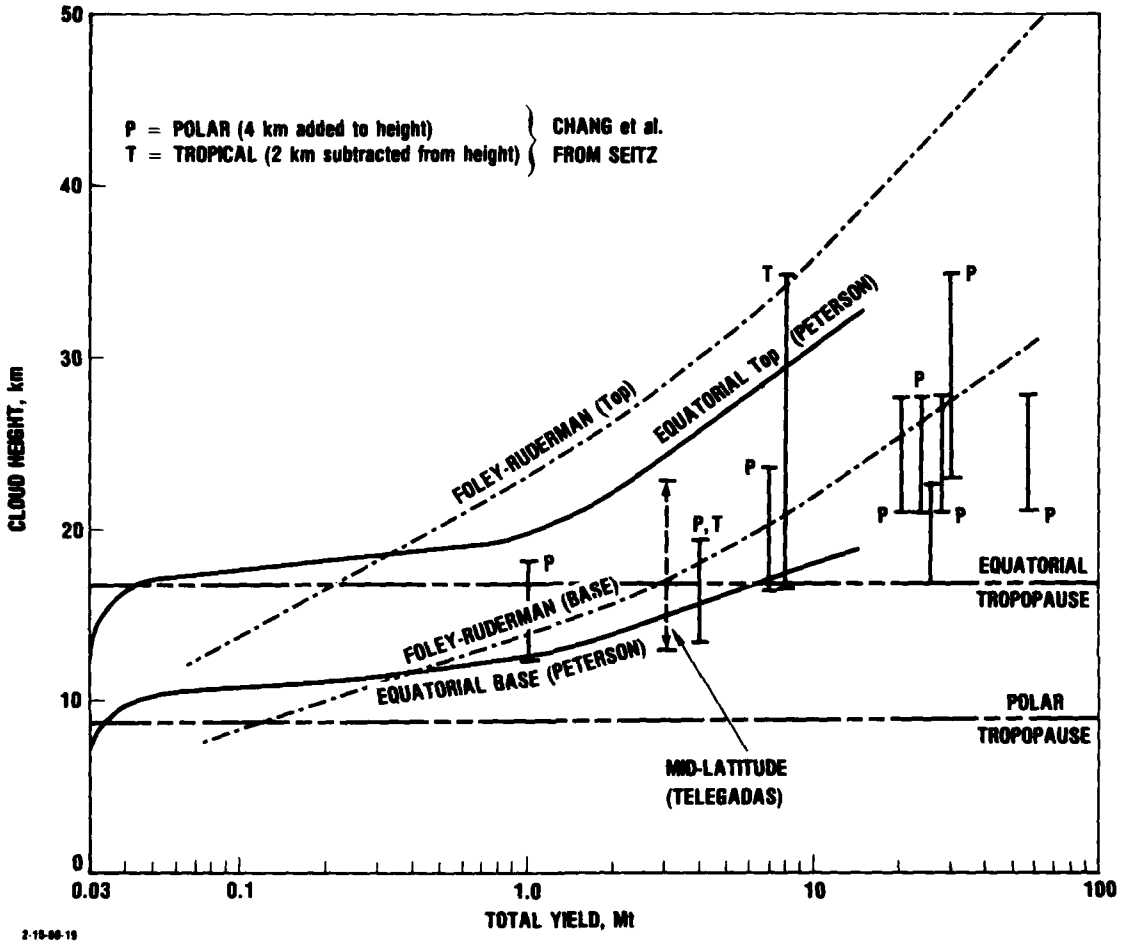

FIGURE 3-1. Nuclear cloud rise height as a function of yield for different latitudes. Peterson's (1970) equatorial model comes from U.S. tests in the tropics and (for low yields) in Nevada (37°N). Foley-Ruderman (1973), from Chang et al. (1979), is an ultrasimplified model which probably gives an upper bound. The vertical lines labeled P or T come from the model of Seitz et al. (1968); the correction for height above the tropopause has been made by Chang et al. (1979) and provides a plausible lower bound for cloud rise. The vertical line labeled "Mid-Latitude (Telegadas)" corresponds to Chinese 3-Mt, 40°N injections (Telegadas 1977).

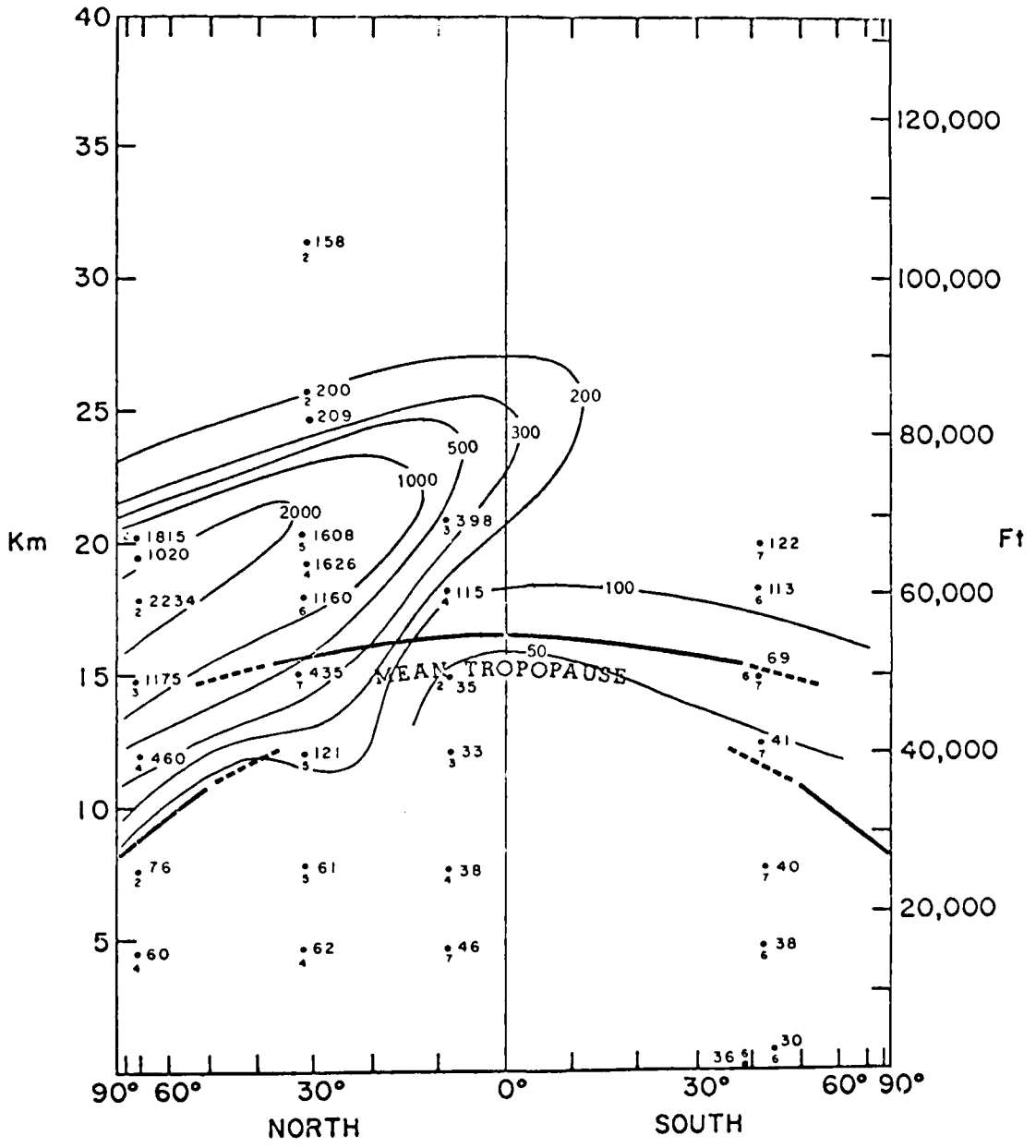

FIGURE 3-2. Atmospheric burden of ^{14}C, December 1962--February 1963, mainly from aircraft sampling. (Source: Telegadas, 1971)

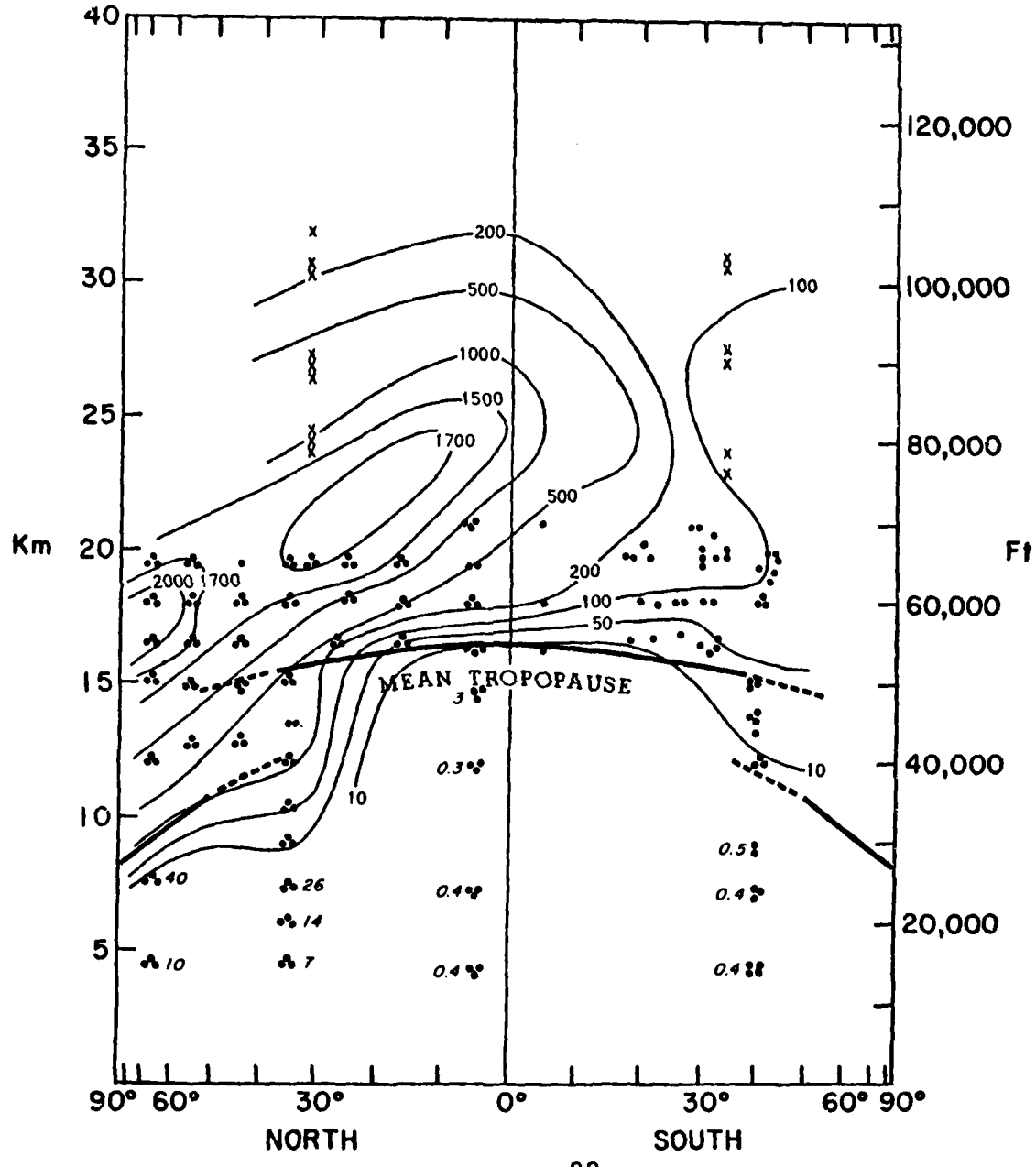

FIGURE 3-3. Atmospheric burden of ^{90}Sr, March-May 1963, mainly from aircraft sampling. (Source: Telegadas, 1968)

approximately 3 Mt) cloud rise is based mainly on aircraft and balloon observations carried out mostly along the west coast of North and South America, or 180° in longitude from the point of injection.

The parameterization of Foley & Ruderman (1973)--see, e.g., Chang et al. (1979)--has also been used. It indicates an extremely high cloud rise for a high-yield bomb; one argument for this comes from the observed enhancement of the lithium airglow following the high-yield Soviet nuclear explosions of October 1961 (Sullivan & Hunten 1964). If the enhanced lithium airglow extends over a horizontal dimension of the order of thousands of kilometers, the observed airglow levels would require several grams of lithium. Since the bomb contained 10-100 kg lithium (Sullivan & Hunten 1964), this observation is hardly convincing evidence that a significant fraction of the cloud rose to very high altitudes.

In view of this uncertainty in injection height, I shall follow the approach of Chang et al. (1979), who use two distinct parameterizations--a high one (Foley & Ruderman) and a low one (Seitz)--which are reduced to an effective mid-latitude injection, as indicated in their paper, by raising the cloud height 4 km for polar tests and by reducing it 2 km for tropical tests. These two parameterizations, which are shown in Fig. 3-1 (after Chang et al. 1979), represent plausible lower and upper bounds. Using these two models for debris injection height and dividing the 1961-1962 injections into five distinct pieces, each with an appropriate mean yield and thus effective injection height, gives the injection groupings listed in Table 3-1. The major stratospheric injections of the 1950s are grouped comparably in Table 3-2.

From Table 3-1 one can infer that for the 1961-1962 test series the effective injection height for ^{14}C, which is a tracer

TABLE 3-1. GROUPING OF INJECTIONS FOR 1961-1962 TEST SERIES[a]

	A: USSR, 13 bombs, 1 Sep - 4 Nov 1961	B: USSR, 2 large bombs, 25 & 58 Mt	C: U.S., 7 bombs, May-Oct 1962	D.1: USSR, 5 bombs, 20-27 Mt, Aug-Dec 1962	D.2: USSR, 11 bombs, 1-10 Mt, Aug-Dec 1962
Mean Injection Date	1 Oct 1961	1 Nov 1961	1 Jul 1962	1 Oct 1962	1 Oct 1962
Total Yield, Mt	37	83	37	125	75
Fraction of Yield	0.110	0.246	0.110	0.371	0.223
Fission Yield, Mt	17	8	11	35[b]	25[b]
Fraction of Fission Yield	0.177	0.083	0.115	0.365	0.260
Mean Yield, Mt	2.8	41.5	5.3	25	6.8
Effective Injection Height, km					
Foley-Ruderman[c]	22	38	25	35	26
Seitz[c]	16	24	19	23	19

[a]Three figures are quoted only to reduce roundoff errors; they do not imply significance.

[b]Total fission yield has been quoted for groups D.1 and D.2 together by Salter (1965); we assume that the ratio of fission yield to total yield is the same for both the "large" and the "small" bombs.

[c]From models of Chang et al. (1979)--see Fig. 3-1.

TABLE 3-2. GROUPING OF INJECTIONS IN THE 1950s[a]

Country/Location	U.S., Tropical	USSR, Mid/High Lat.	USSR, Mid/High Lat.	U.S. & U.K., Tropical	USSR, Arctic
Mean Injection Date	Jun 1956	Sep 1956	Jun 1957	Jun 1958	Oct 1958
Total Yield,[b] Mt	10.5	6	12	21	36
No. of Bombs	5	4	5	30	10
Effective Injection Height, km					
Foley-Ruderman	21	20	21	17	23
Seitz	15	16	16	15	16

[a]Stratospheric injections of 1952-1954 were small.

[b]This is the effective yield that entered the stratosphere, i.e., yield of air bursts plus half yield of surface bursts (K. Telegadas, personal communication).

of total yield, was some 1 to 2 km greater than that of ^{90}Sr, which is a tracer of fission yield, mainly because the Soviet 58-Mt bomb of 30 October 1961 had a very low fractional fission yield.

In closing, note that the available information on cloud rise height for the large Soviet bombs of 1961-1962 is based on limited and indirect data and should be used with extreme caution.

4. EDDY DIFFUSIVITY PROFILES

Figure 4-1 and Table 4-1 show some eddy diffusivity or K-profiles that have been used in one-dimensional (1-D) modeling of stratospheric photochemistry between 1974 and the present. The following points should be noted:

- The atmosphere is three-dimensional, and actual transport is a complex combination of convective and diffusive motions, with a great deal of space and time variability. To parameterize this complexity in terms of down-gradient diffusive transport with simply one parameter, $K = K(z)$, which depends only on height, is clearly an oversimplification. The 1-D parameterization has been used extensively in describing problems which are largely determined by chemistry but where the dynamics must be inserted in the simplest feasible way. It is relatively satisfactory for processes that take place sufficiently far above the local tropopause, perhaps at 18 to 20 km, for details in the region of the tropopause to be unimportant. In the application to present-day aircraft injections which often take place near the local tropopause, so that the aircraft sometimes fly in tropospheric air (high moisture, low ozone) and sometimes in stratospheric air (low moisture, high ozone), the concept of a 1-D model associated with a K-profile must be used with extreme caution.
- A variety of different K-profiles have been suggested by different workers (Fig. 4-1 and Table 4-1). They

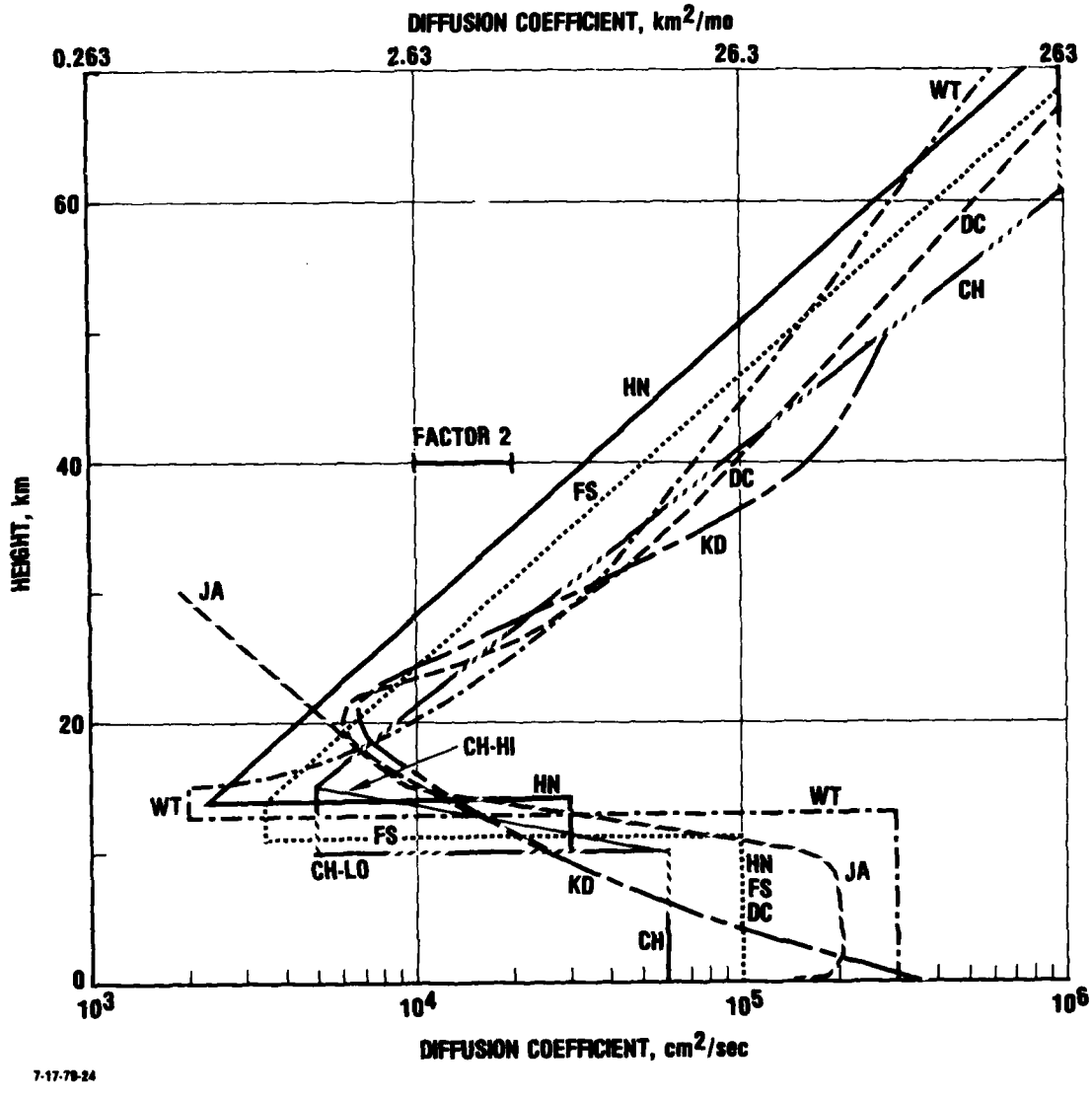

FIGURE 4-1. One-dimensional eddy diffusivity profiles. See Table 4-1 for explanation.

TABLE 4-1. SOME K-PROFILES USED FOR STRATOSPHERIC PHOTOCHEMISTRY

Code	Name	Reference (for numbers used here)	Principal Tracer Used for Upper Stratosphere	Tropopause Height, km	"Tropopause Region," km	Characteristics of the Profile
CH-HI	Crutzen-Howard	Crutzen and Howard (1978)	N_2O	10	10-15	Fairly rapid transport out of lower stratosphere
CH-LO	Crutzen-Howard	Crutzen and Howard (1978)	N_2O	10	10-15	Fairly slow transport
DC	Dickinson-Chang	Poppoff et al. (1978)	CH_4 & N_2O	10	10-15	Rapid transport, minimum at high altitude (> 20 km)
FS	Wofsy	Bauer and Gardner (1977)	CH_4	11	11-14	Slow transport
HN	Hunten	Bauer and Gardner (1977)	CH_4	10	10-14	Slowest transport (except for WT) that has been suggested seriously; original recommendation was to increase effective injection height by 2 km for aircraft
WT	"Wofsy-Type" or "Whitten-Turco"	Poppoff et al. (1977)	CH_4	13	13-15	Very low minimum gives slow transport
KD	Danielsen	ms, 1979	O_3, N_2O 3-D Model	11	11-15	Rapid transport except in the upper troposphere
JA	Jacobi-André	Jacobi and André (1963)	^{222}Rn, ^{220}Rn and decay products			Emphasizes planetary boundary layer ($\lesssim$ 1-2 km) but extends into lower stratosphere

all show similar qualitative characteristics--fast transport in the upper stratosphere and in the troposphere, with a minimum between the tropopause and altitudes of 18 to 25 km. The shape and magnitude of this minimum are critical in determining how fast a tracer injected in the middle or upper stratosphere ($\gtrsim$20 km) is swept out to a sink at the ground; radioactive tracer data provide relatively direct information on this minimum.

- Note that the "slow" profiles such as WT and HN have a very low minimum K-value and thus provide only slow transport out of the stratosphere. In contrast, the "fast" profiles DC and KD have a relatively large minimum and so produce a minimum barrier to transport out of the stratosphere.

- The profile "JA"--from Jacobi and André (1963)--was devised to explain the behavior of fallout products in the planetary boundary layer ($z \lesssim 1$ to 2 km) and to some extent in the free troposphere. It was certainly not intended to be used in the stratosphere, but as one sees in Fig. 4-1, its behavior below 20 km is not inconsistent with some other profiles, especially DC and KD.

- The rise in K-values above 15 to 20 km and up to 40 to 50 km, in many cases, depends on the N_2O profiles of Schmeltekopf et al. (1977) and on the loss mechanisms of N_2O, which are believed to be approximately 80 percent by photolysis with solar UV below 230 nm, and 20 percent by reaction with $O(^1D)$, about half of which produces NO. The older estimates of K(z) based on methane profiles depend on the assumed loss rate by reaction with OH and $O(^1D)$ in a chlorine-free atmosphere; the loss rate varies with the ambient chlorine concentration, among other factors. There is also the

fundamental point that the K-profile depends on the loss rate of the tracer, which depends on the model of photochemistry for a reactive tracer.

- The most recent discussion is that of Danielsen (1979), who uses three very different tracers (ozone, nitrous oxide, and the results of a three-dimensional computer simulation) and derives a profile "KD", which in his opinion has an overall uncertainty of a factor of two.
- Except in the critical 10-20 km region, few of the K-profiles differ by more than a factor of two.
- In the present one-dimensional analysis, the primary quantity to be modeled is the time-dependence of the stratospheric burden of an injectant. For this I use the representative description of Telegadas (1971), in which the stratosphere is taken as containing 20 percent of the atmospheric mass, giving a global mean tropopause height of 11 km. Note that Ellsaesser (1975), p. 7-13, suggests a stratospheric mass of 6.67×10^{17} kg versus Telegadas' 1.02×10^{18} kg, or 15 percent of the total atmospheric mass, which would correspond to a global mean tropopause height of approximately 13 km.

5. THE DIFFUSION MODEL

5.1. MATHEMATICAL FORMALISM

The atmosphere is characterized by a number density $n = n(z)$ which depends on height z; under isothermal conditions (approximately true between 11 and 20 km), one has

$$n(z) = n(z_o) \exp [-(z-z_o)/H], \qquad (5.1)$$

where the scale height $H = kT/Mg = 6.3$ km in the 11-18 km region, where $T = 217^{\circ}K$. Atmospheric dynamics is parameterized in terms of the $K(z)$ profile discussed in Section 4, while aerosols are characterized by a sedimentation speed $u = u(z)$ (see Section 5.3).

One is dealing with chemically inert tracers characterized by a globally averaged mixing ratio

$$f(z,t) = \frac{\text{burden of tracer between } z \text{ and } (z + \Delta z) \text{ at time } t}{\text{air mass between } z \text{ and } (z + \Delta z)}, \qquad (5.2)$$

$f(z,t)$ being a solution of the following diffusion equation:

$$(\partial/\partial z) [n(z)K(z)\partial f/\partial z + n(z)u(z)f(z,t)] = n(z)\partial f/\partial t. \qquad (5.3)$$

The differential equation (Eq. 5-3) has to be solved for appropriate initial conditions discussed in Section 5.2 and for boundary conditions discussed in Section 5.4. An analytic solution for a simplified K-profile was given earlier (Bauer, Oliver, Wasylkiwskyj, 1978); the problem is here solved numerically, and the integration scheme is outlined in Section 5.5 and discussed in detail in Bauer (1980), which is available on request.

5.2. INITIAL CONDITIONS

For the Chinese explosions it is assumed that the mean injection height is approximately 18 km, corresponding to the mid-latitude injection of a 3-Mt bomb. Figure 3-4 shows the vertical ^{95}Zr activity distribution for five of the six Chinese high-yield explosions; note that this is not a direct observation, but rather has been reconstructed largely from the Airstream observations flown halfway around the globe from the point of injection. From the discussion of Telegadas (1977), it is possible to assume an initial distribution for the mixing ratio f(z,t) of Gaussian form

$$f(z,0) = f_o \exp\left[-(z-z_1)^2/\sigma_o^2\right] \quad , \qquad (5.4)$$

where z_1 = 18 km and σ_o = 2.15 km.

The model of Eq. 5.4 is believed to be adequate for a mid-latitude 3-Mt bomb, which corresponds to four of the six Chinese high-yield tests. The other two Chinese tests had, respectively, a yield of "2 to 3 Mt" (June 1973) and "4 Mt" (November 1976) (see Table 2-1), and to a first approximation one may again use the model of Eq. 5.4.

For the Soviet and U.S. atmospheric nuclear explosions of 1961 to 1962, for which the yield and also the latitude and season of injection varied significantly, I make estimates of injection height using the Foley-Ruderman and Seitz models of Section 3. Note:

- For a given injection of Table 3-1 or 3-2, the distribution of debris mixing ratio is described by a Gaussian model like Eq. 5.4 with mean injection height z_o, the mean of the lower and upper bounds of total activity from Fig. 3-1, and with σ_o = 2.15 km, as for the Chinese 3-Mt tests. (The choice of injection heights has been discussed in Section 3; I use both "low" (Seitz) and

"high" (Foley-Ruderman) values. It would be possible to use different values of σ_o, such as one-fourth of the spacing of lower and upper bounds of Fig. 3-1, which would give values ranging from 1.7 km (Seitz, case A of Table 3-1) to 4.2 km (Foley-Ruderman, case B of Table 3-2). Unlike the choice of injection height, the choice of σ_o is not critical, since we are asking for the total burden of ^{90}Sr and $^{14}CO_2$ a long time after the injection, and thus the injection height and the total amount of material injected are far more important than the details of the initial distribution function, which is smeared out fairly rapidly.

- For the U.S. and Soviet injections of 1961 and 1962, a lumped model, replacing the 28 distinct explosions by five separate injections, is developed in Section 3 (see Table 3-1 and also Table 3-2 for stratospheric injections of the 1950s). In effect, a series of injections at a given time, location, and altitude is combined to produce a single averaged injection. Referring to Table 3-1, group A corresponds to 13 Soviet bombs of yield in the 1- to 3-Mt range detonated between 1 September 1961 and 4 November 1961, and so on. For all the groupings except B, the ratio of fission yield/total yield is essentially the same, 1/3. Group B, consisting of two very large Soviet detonations (25 and 58 Mt) had a very small ratio of fission yield/total yield, approximately 0.1, and as a result of this group--more or less of the single 58-Mt bomb--the effective injection height of ^{14}C (which is proportional to total yield) is approximately 1 to 2 km higher than that of ^{90}Sr, which is proportional to fission yield.
- For ^{14}C it is necessary to include the earlier nuclear explosions to simulate the behavior after 1963. The various injections from 1956 to 1958 are simulated by five different injections listed in Table 3-2.

5.3. SEDIMENTATION OF AEROSOLS

^{90}Sr and ^{95}Zr are carried on stratospheric aerosols, submicron particles composed mainly of H_2SO_4-H_2O mixtures deposited on various condensation nuclei. These aerosols make up the "Junge layer" of submicron particles, mainly in the 18-20 km lower stratosphere altitude region. The particles are in dynamic equilibrium; photochemical formation of H_2SO_4 from sulfur compounds diffusing up from the troposphere (SO_2 and COS, mainly) and reacting with OH and HO_2 radicals in the stratosphere is followed by a variety of physical processes of condensation, evaporation, coagulation, sedimentation, and diffusion. The most recent and comprehensive model of the Junge layer has been given by Turco et al. (1979) and Toon et al. (1979); see also Hamill et al. (1977), who discuss the physics but not the photochemical production mechanisms.

The average of a surface- and volume-weighted mean of the particle size distribution computed by Turco et al. (1979) is 0.3 μm, but Drevinsky & Pecci (1965) found that most of the radioactivity is carried on particles of 0.02-0.15 μm radius.

Here I assume a rate of sedimentation corresponding to spherical particles of radius 0.1 μm (as did Telegadas & List, 1969), with mean density of approximately 1.8 g/cm^3 (corresponding to saturated H_2SO_4/H_2O droplets at these altitudes). I do not know how to include the effects of all the physics in the recent models listed at the beginning of this section in a fallout parameterization.

A natural question to ask is how significant the effect of sedimentation is in the present context. Spherical particles of radius 0.1 μm and density 1.8 g/cm^3 have a sedimentation speed u = 0.0032 cm/sec = 0.08 km/month at an altitude of 18 km (see Kasten 1968, whose velocity profile differs slightly from

the earlier one of Junge et al., 1961). For injection at some height z_1 in the 18 to 20 km altitude range, an aerosol of this size is transported out of the stratosphere approximately as fast as a gas injected at a height 1-2 km lower. However, for long-term falloff, the effect of the lower boundary condition, which is taken up in the next section, is more significant than that of sedimentation.

5.4. BOUNDARY CONDITIONS

In the numerical integration of the diffusion equation (Eq. 5.3) one has injections of material around z = 20 km, and the integration extends from z = 0 (ground) to z = 50 km. The choice of boundary conditions is critical for the integration and differs for different tracers. At the upper boundary, the proper condition to choose is one of no net flux across it. The flux is obtained by integrating Eq. 5.3 with respect to z for the flux density:

$$\text{Net flux} = nK\partial f/\partial z + nuf. \qquad (5.5)$$

For the case of a gas, with no sedimentation so that u = 0, the boundary condition of no net flux is

$$\partial f/\partial z = 0 \text{ at upper boundary.} \qquad (5.6)$$

There are two distinct cases for the lower boundary condition.

5.4.1. Perfect Sink at Bottom

This condition is appropriate for fission fragments (^{90}Sr and ^{95}Zr) and also for HTO or H_2O which are not recycled rapidly once they reach the ground, and it is

$$f = 0 \text{ at lower boundary/surface.} \qquad (5.7)$$

5.4.2. Finite Loss Rate at Bottom

This condition is appropriate for $^{14}CO_2$, which is only absorbed rather slowly by the ocean (see, e.g., Machta, 1973).

There is an effective loss velocity v_e characterized as follows:

$$nK\partial f/\partial z + nuf = nv_e f \text{ at lower boundary.} \qquad (5.8)$$

The value of v_e for $^{14}CO_2$ is obtained as follows. Machta (1973), Fig. 2, quotes a tropospheric mass of CO_2 of 6×10^{17} g, and in a box model, a transfer rate into the ocean of 0.22 $year^{-1}$ (also back transfer from ocean to atmosphere of 0.1 $year^{-1}$). Now the concentration of $^{14}CO_2$ in the atmosphere after the nuclear tests was far greater than in the ocean, and thus back transfer should be neglected, so that the mass transfer rate = $6 \times 10^{17} \times 0.22$ g/year = 4.18×10^9 g/sec. The density of CO_2 at the surface is

$$\rho_{CO_2} = 1.225 \times 10^{-3} \times 3.3 \times 10^{-4} \text{ g/cm}^3 = 4.04 \times 10^{-7} \text{ g/cm}^3.$$

Now if the effective surface area is A, then the deposition speed v_e is given by the relation

$$\text{mass transfer rate} = \rho_{CO_2} A v_e. \qquad (5.9)$$

Taking A = total surface area of earth = 5.11×10^{18} cm^2 gives v_e = 0.00202 cm/sec = 0.053 km/month, which is the value to be used here for $^{14}CO_2$. If one considers that most of the exchange takes place with the ocean, which covers two-thirds of the surface of the earth, the actual exchange velocity with the ocean is (3/2) x 0.053 km/month = 0.08 km/month. However, this is not the appropriate velocity to be used here, since we are dealing with a global mean velocity.

5.5. THE NUMERICAL MODEL

The left-hand side of Eq. 5.3 contains two terms:

$$\left.\begin{aligned} T_1 &= (\partial/\partial z)\ (nK\partial f/\partial z) \qquad \text{(a)} \\ T_2 &= (\partial/\partial z)\ (nuf). \qquad \text{(b)} \end{aligned}\right\} \qquad (5.10)$$

Because here T_1 is more important than T_2, the problem is the integration of a parabolic partial differential equation, for which the ordinary explicit numerical integration scheme becomes unstable unless

$$2\,\bar{K}\Delta t/(\Delta z)^2 \leq 1. \qquad (5.11)$$

It is appropriate to use spatial steps of Δz = 1 km (note also that the K-profiles that are normally used have discontinuities, which may cause further difficulties), and because the actual K-values are of the order of 10^4 cm^2/sec (2.63 km^2/month) in the lower stratosphere, or 10^5 cm^2/sec (26.3 km^2/month) in the troposphere and upper stratosphere, the condition of Eq. 5.11 requires a time step as small as Δt = 0.01 month for stability if one uses an explicit scheme. With the implicit Crank-Nicholson scheme, which is customarily used for parabolic equations of this type (see, e.g., McCracken & Dorn, 1964, pp. 365-404; Richtmyer & Morton, 1967, pp. 185-201), a time step Δt = 1 month gives stable and accurate results, as checked against the analytic two-step solution of Wasylkiwskyj (see Bauer, Oliver, & Wasylkiwskyj, 1978, and Bauer, 1980, item 3). With a time step Δt = 1 month, running for times t = 20 months, the program takes several seconds to run on IDA's CDC-6400. Times as long as t = 15 years are needed for simulation of the 1961-1962 test series, and thus it is evident that an explicit scheme, with a time step Δt = 0.01 month, would be extremely time consuming and subject to large roundoff errors in addition to possible errors associated with discontinuities in the K-profile. The implicit Crank-Nicholson scheme is stable and accurate. A complete documentation of the computer program is given in Bauer (1980), which is available on request.

5.6. IMPULSIVE VERSUS STEADY-STATE INJECTIONS: A COMPARISON OF ATMOSPHERIC RESIDENCE TIMES

One may ask for the relation between the present model for an impulsive injection and the case of a steady-state strato-

spheric injection, such as that due to aircraft. For a steady-state injection, one may define an atmospheric residence time

$$T_{ss} = \text{flux/burden} \qquad (5.12)$$

(see, e.g., Bauer & Gardner, 1977). For the present case one may define a residence time T_{imp} in terms of the time-dependent stratospheric burden B_{strat},

$$B_{strat}(t_1 + T_{imp}) = (1/e)\, B_{strat}(t_1), \qquad (5.13)$$

i.e., as that time in which the stratospheric burden falls to 1/e of its value at some initial time t_1.

Some numerical examples for an 18-km injection and a DC profile are given in Table 5-1, which shows that for this case there is a significant variation in T_{imp} as t_1 changes. (Note that for a "slow" profile like WT much less variation in T_{imp} would be detectable over the 50-month run from which the estimates of Table 5-1 were made.)

TABLE 5-1. STRATOSPHERIC RESIDENCE TIMES FOR STEADY STATE AND IMPULSIVE INJECTIONS

(K-profile: DC, 18-km injection of a gas, no recycling at ground)

Steady State, Eq. 5.12:

T_{ss} = 18.9 months (Bauer and Gardner, 1977, p. D-19)

Impulsive Case, Eq. 5.13:

Initial Time t_1, months	Residence Time, T_{imp}, months
0	12.1
5	13.6
10	18.9
15	23.8
20	27.2

In conclusion, it should be noted that while one K-profile may be applied to a steady or impulsive injection at arbitrary heights and be used to describe the parameterized dynamics, yet an atmospheric residence time can be defined in different ways which may give different numerical values even if the underlying dynamics, i.e., the K-profile, are the same.*

*For a detailed discussion of various definitions of residence times under steady and unsteady state conditions, see, e.g., Schwartz (1979).

6. COMPARISON OF THE DATA WITH CALCULATIONS

6.1. INTRODUCTION

Section 6.2 compares the decline in stratospheric burdens of ^{95}Zr from several Chinese thermonuclear explosions with model predictions. Section 6.3 treats the decline in stratospheric burden of ^{90}Sr following the 1961-1962 injections, while Section 6.4 considers the time variation in excess $^{14}CO_2$ through 1969; because of the slow loss rate of $^{14}CO_2$ to the ground (mainly into the ocean), it is necessary to consider injections from the 1950s (Table 3-2) as well as the larger injections from 1961-1962 (Table 3-1).

These analyses of the decay in stratospheric burden with time require that the initial injection height of the tracers should be known. Especially for the Soviet bombs (which contributed 90% of total yield during the 1961-1962 time period) the injection heights are not well known (see Section 3 for a discussion of the problem), and thus in Section 6.5 I adopt an alternative approach which was first used by Johnston, Kattenhorn & Whitten (1976), who analyzed the time variation of the altitude profiles of ^{90}Sr and $^{14}CO_2$. My conclusions are rather different from those of Johnston et al., and this is traced back to the boundary conditions used.

6.2. CHINESE BOMBS: ^{95}Zr DATA, 1967-1978

The discussion of Section 2.3, and in particular Fig. 2-6, shows that when the decay-corrected stratospheric burdens of ^{95}Zr are normalized and compared on a seasonally adjusted basis, they show slow fallout until the first winter season and fairly rapid fallout thereafter.

Figure 6-1 compares calculations with the observed and suitably normalized ^{95}Zr data. The calculations all assume a mean injection at 18 km (see Eq. 5.4 for the initial condition assumed) and the following boundary conditions for the mixing ratio f(z,t) (Eq. 5.2):

Perfect sink at the bottom, i.e., $f(z = 0,t) = 0$ (6.1)

No flux through the top (Section 5.4), (6.2)

which are appropriate for this precipitation scavengeable tracer.

I assume sedimentation (see Section 5.3 for the model used), and injections on 1 January and 1 July for fast transport (K_{DC}) and slow transport (K_{WT}), respectively.

Overall, fast transport for a January injection, or after a delay until the first winter following a summer/fall injection, provides an adequate representation of the data.

6.3. ^{90}Sr DATA, 1960-1967

If one looks at Fig. 2-7, one sees that in comparison with ^{14}C the stratospheric burden of ^{90}Sr decays rather rapidly with time, and so in analyzing the data it is not necessary to correct for injections during the 1950s. The injection of the 1961 to 1962 test series is modeled in terms of the five distinct injections shown in Table 3-1. Figure 6-2 compares the stratospheric ^{90}Sr burden from Fig. 2-5 with model calculations using the DC and WT profiles of Section 4 (with the effects of sedimentation included), and with the "Foley-Ruderman" (high) and "Seitz" (low) cloud rise estimates as used by Chang et al. (1979). The absolute magnitude of the computed burden is fitted to the observed activity in January 1963.

One sees that the fast DC transport with the low (S) cloud rise height fits the decay of ^{90}Sr after January 1963 far better than any other combination. Fast transport is consistent with

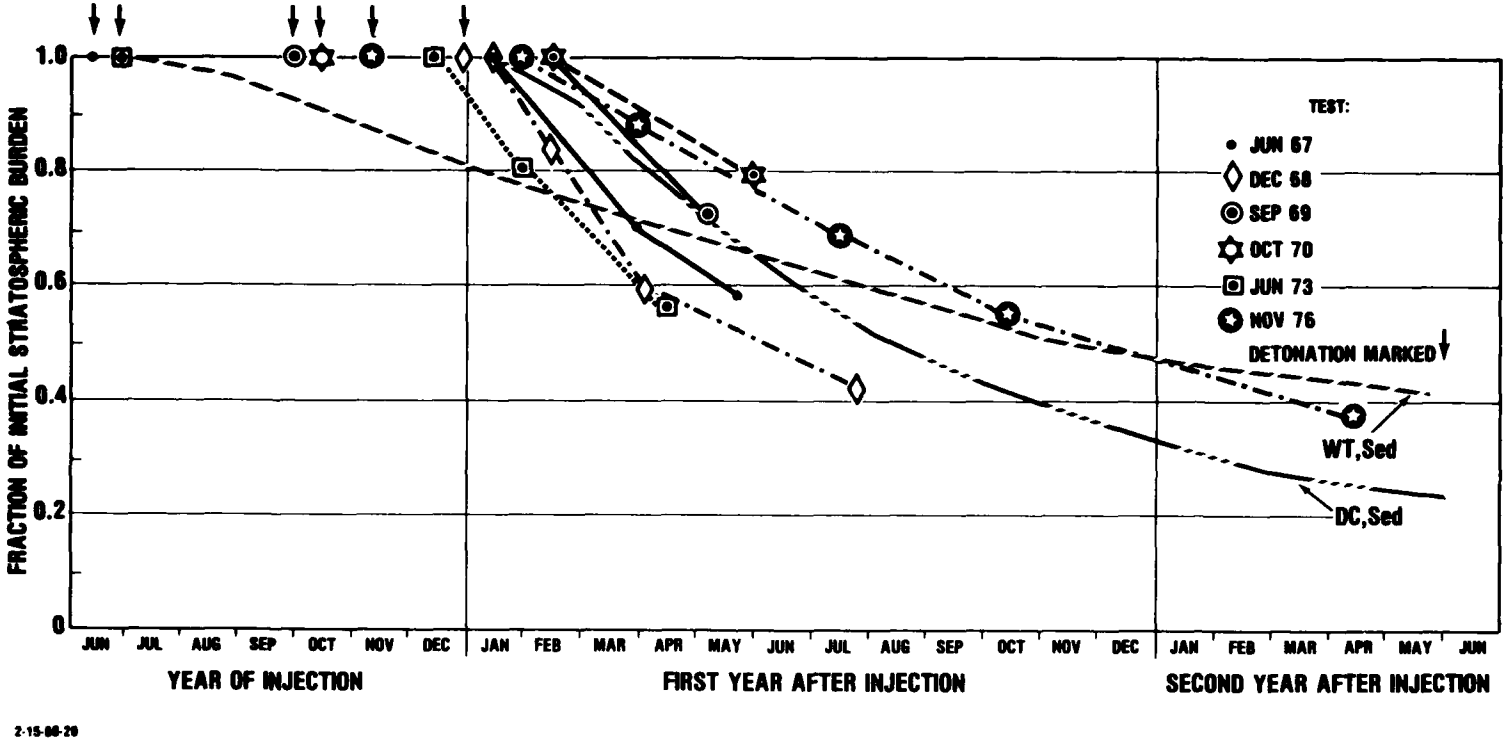

FIGURE 6-1. Comparison of calculations with observed and suitably normalized ^{95}Zr data.

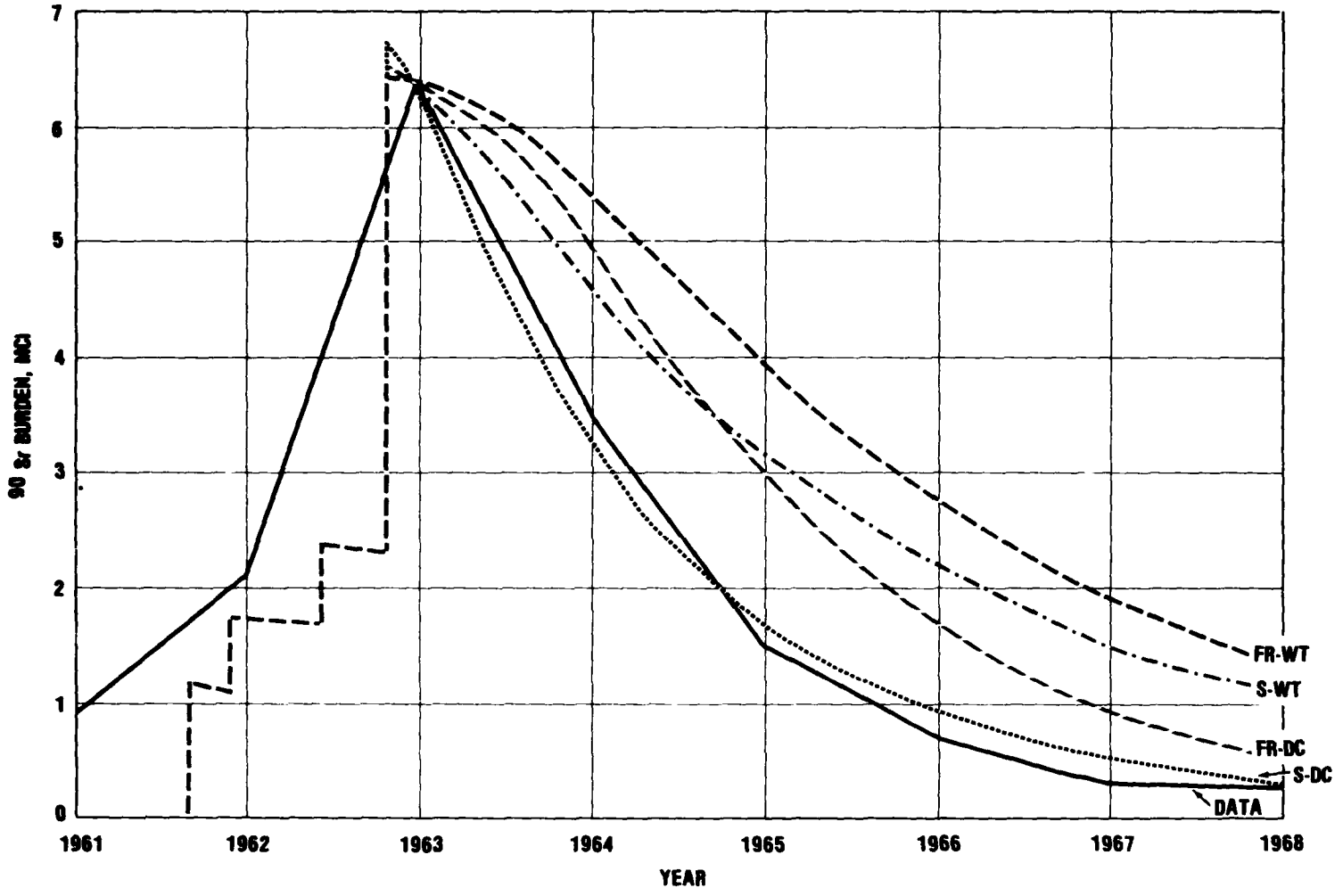

2-15-88-21

FIGURE 6-2. Decrease in stratospheric burden of ^{90}Sr following the 1961-1962 injections. We show results for "high" (FR) and "low" (S) injection heights (Section 3), and for "fast" (DC) and "slow" (WT) transport (Section 4). The calculated burden is matched with the measured burden in January 1963.

the ^{95}Zr results, since the Soviet injections took place in late fall, so that the fast winter transport took over shortly after the injection. Regarding the cloud rise, evidently the lower the injection height, the faster the removal for a given K-profile, and certainly the Airstream data offers no evidence for the FR (high) cloud rise.

After 1967, the effects of Chinese and French nuclear explosions raised the ^{90}Sr level to a detectable extent, so the present comparison terminates there.

6.4. ^{14}C DATA, 1958-1969

Reference to Fig. 2-7 shows that in comparison with ^{90}Sr, which falls out of the stratosphere rather rapidly and is rained out of the troposphere so that its tropospheric burden is very small, ^{14}C, which is found in the atmosphere as CO_2, stays much longer. While the higher injection height of ^{14}C and the sedimentation of ^{90}Sr do have an effect, the principal cause of this has to do with the lower boundary condition: $^{14}CO_2$ is only lost very slowly at the surface--mean disappearance time 4.5 years (see Machta 1973)--and is present in the troposphere for a number of years after stratospheric injection (Fig. 2-9). Thus the lower boundary condition for $^{14}CO_2$ is quite different from that for any of the other tracers considered here. See Section 5.4.2 for a discussion.

Because of the long atmospheric residence time of $^{14}CO_2$, if one wishes to study the effects of ^{14}C injections in 1961-1962, it is necessary to consider the injections of the 1950s (Table 3-2) as well as the 1961-1962 injections, which are parameterized as shown in Table 3-1. The earlier injections provide a background for the 1961-1962 tests, and thus I compare results between 1958 and 1969, after which the effects of French and Chinese explosions obscure the record.

The data of Fig. 2-6 over the period 1958-1969 are thus compared with the results of the present simulation, using the high (FR) and low (S) injection heights of Section 3 and the "fast" (DC) and "slow" (WT) K-profiles of Section 4. Figure 6-3a shows calculations for high injection height ("Foley-Ruderman" of Section 3, or FR), and Fig. 6-3b shows the results for low injection height ("Seitz" of Section 3, or S). One sees that:

- The high-altitude injection gives too slow a decrease in the stratospheric burden of excess ^{14}C and also too late and too small a maximum in the tropospheric burden.
- The low injection height with a "fast" transport coefficient K_{DC} reproduces both the observed decrease in stratospheric burden and also the peaking in tropospheric ^{14}C.

6.5. ANALYSIS OF ALTITUDE PROFILES OF ^{14}C: DIFFERENCES BETWEEN THE ANALYSIS OF JOHNSTON, KATTENHORN, AND WHITTEN (1976) AND THE PRESENT WORK

Johnston, Kattenhorn & Whitten (1976) took the altitude-latitude network of excess ^{14}C data from 1963 to 1969 (Telegadas 1971) and constructed a Northern Hemisphere mean altitude profile of both number density and mixing ratio at various times. They found that this Northern Hemisphere mean (corrected for leakage to the Southern Hemisphere) agrees well with the observed profile from $30^{\circ}N$, so that in this instance two representations used for a 1-D parameterization agree. They used a numerical diffusion equation to test how well different K-profiles were able to reproduce the changing altitude profile of ^{14}C, mainly on a year-by-year basis, but also over longer times; and they found that the Hunten (HN) profile, a fairly slow K-profile, reproduces most of the data better than any of the other K-profiles they considered.

Their boundary conditions are described in their paper as follows: "The lower boundary condition was that observed at

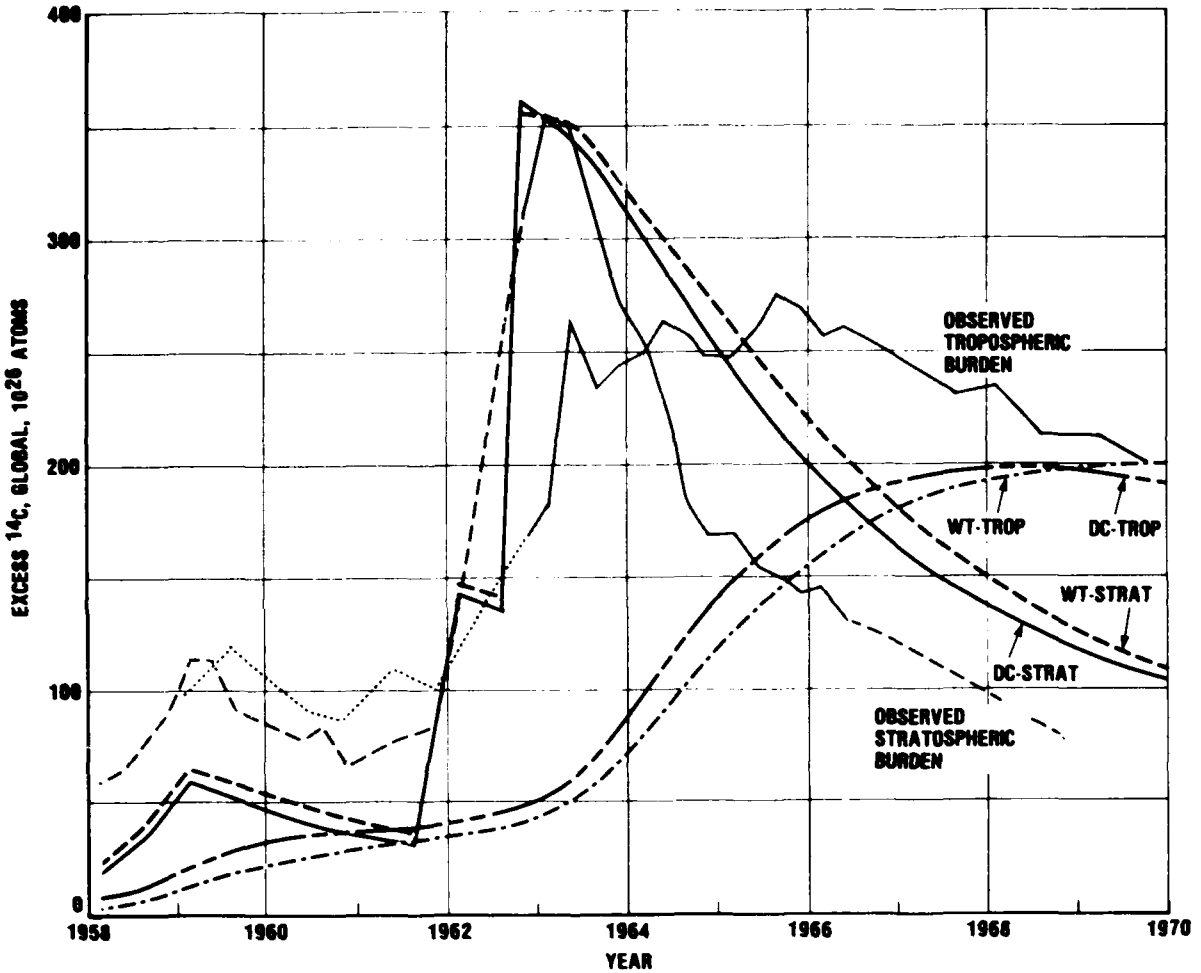

FIGURE 6-3a. Calculations of excess ^{14}C in stratosphere and troposphere. High (FR) injection height.

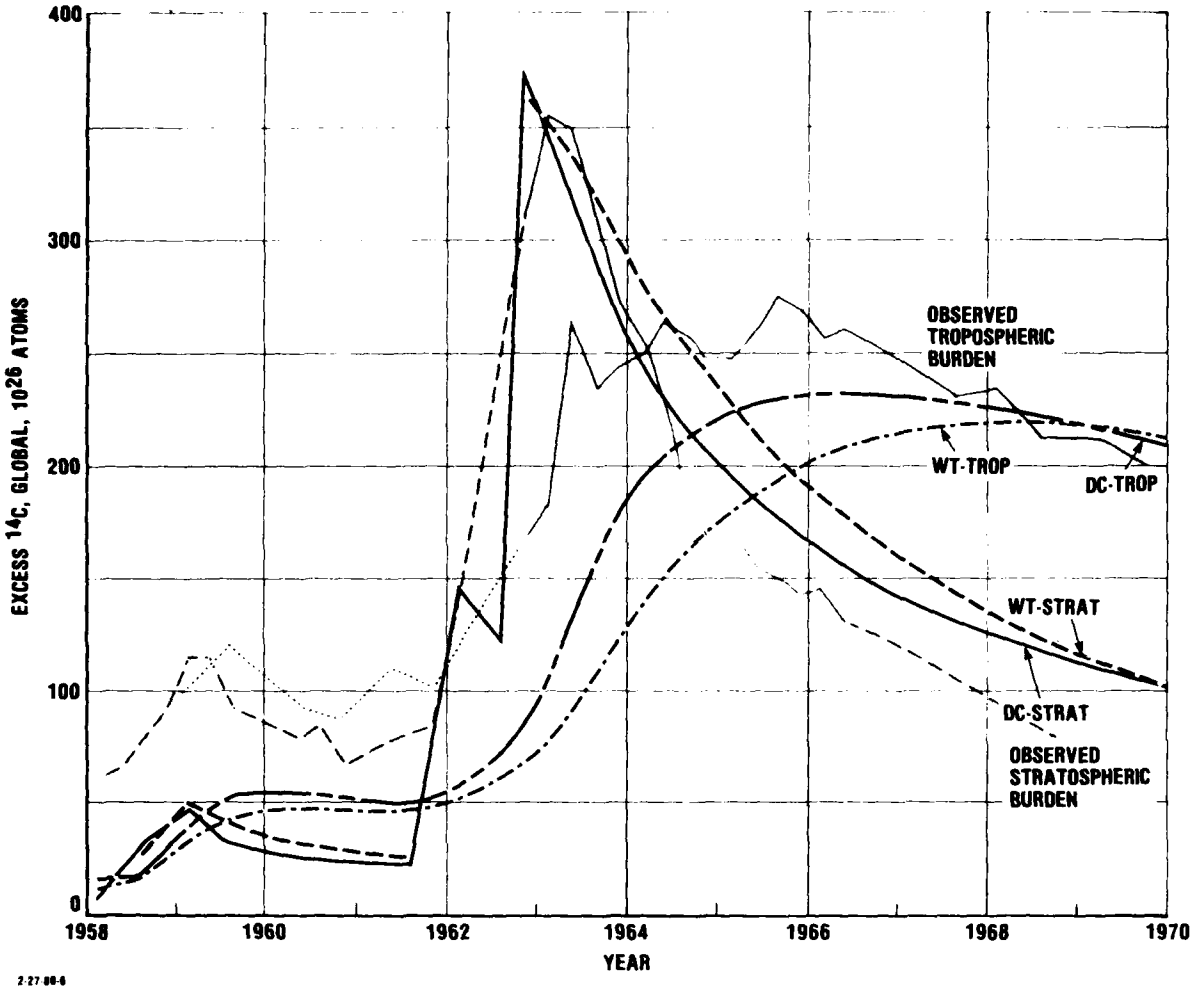

FIGURE 6-3b. Calculations of excess ^{14}C in stratosphere and troposphere. Low (Seitz) injection height.

1 km, which remained constant for several years near 3×10^{-16} mixing ratio. The upper boundary condition was that the concentration at 51 km was one half that at 50 km."

These boundary conditions are not appropriate for ^{14}C or $^{14}CO_2$, because they are equivalent to very strong sinks at both the upper and lower boundaries.

Consider first the lower boundary. In the present notation, the mixing ratio at the bottom step is $f_1 = c$ = constant (3×10^{-16}). This means that there is a very strong sink at $z = 1$ km because any material that comes to the bottom step, tending to change f_1 from the value c, is immediately absorbed. Formally, the mixing ratio $f(z,t)$ is a solution of a linear (diffusion) equation, Eq. 5.3, which one may write

$$L(f) = 0. \tag{6.3}$$

Now, let

$$f(z,t) = c + g(z,t). \tag{6.4}$$

Then, since c is a constant, $L(c) = 0$, and thus $g(z,t)$ is a solution of the diffusion equation, one has $L(g) = 0$. Thus an equivalent way of describing what is done is to solve the diffusion equation $L(g) = 0$ with the lower boundary condition

$$g_1 = f_1 - c = 0 \tag{6.5}$$

and then to add the constant c to the profile at all altitudes. The boundary condition of Eq. 6.5 is appropriate for a tracer such as ^{90}Sr or ^{95}Zr which is precipitation scavenged and lost on the ground, but not for $^{14}CO_2$, for which the discussion of Section 5.4.2 shows that a much weaker sink exists at the bottom: explicitly, Eq. 5.8 shows that the lower boundary condition is

$$\partial f/\partial z = v_e f/K_b \ , \tag{6.6}$$

where $v_e = 0.053$ km/month, and $K_b \sim 25$ km^2/month.

The upper boundary condition

$$f_{51} = \frac{1}{2} f_{50} \tag{6.7}$$

defines a net sink at the top, because

$$\text{grad } f = \partial f/\partial z = (f_{51}-f_{50})/(\Delta z) = - f_{50}/2(\Delta z) = - v_{ee} f/K_t, \tag{6.8}$$

where now $v_{ee} = K_t/2(\Delta z) \sim 10$ km/month. It can readily be shown (see, e.g., item 3 of Bauer 1980) that this boundary condition corresponds to a very strong sink, approximately equivalent to a "perfect sink" $f_{50} = 0$. (The transformation $f = g + c$ changes the numerics a little, but not the essence of the argument.)

As a consequence of these boundary conditions, Johnston et al. (1976) have a source of $^{14}CO_2$ at approximately 20 km and study the loss of material to sinks at the ground (1 km) and also at the stratopause (50 km). Because these sinks are unphysically strong for $^{14}CO_2$, they must have unphysically slow transport between the source and the sinks to reproduce the observed concentration profile.

Johnston et al. (1976) reinitialize their concentration profile at annual intervals, which reduces the effects of the boundary conditions and of leakage to the Southern Hemisphere, but which can lead to incorrect conclusions if there is a change in effective K-profile with time such as was found by Mahlman (1975) in a 3-D numerical simulation.

I have done calculations similar to those of Johnston et al., using their initial profile of January 1963 (see their Table 5) in the form

$$f_{ic}(z) = f_{co}\exp\left[-(z-z_c)^2/\sigma_c^2\right], \tag{6.9}$$

where $f_{co} = 91.5\text{x}10^{-16}$, $z_c = 21.4$ km, $\sigma_c = 3.65$ km, and all permutations of the following boundary conditions are used:

Upper boundary: (a) no flux, $\partial f/\partial z = 0$

(b) perfect sink, $f = 0$

Lower boundary: (a) proper boundary condition for ^{14}C, i.e., Eq. 6.6

(b) perfect sink, $f = 0$.

Note that these conditions are not identical with those of Johnston et al., but they are very similar.

Some representative mixing ratio profiles are shown in Fig. 6-4 for January 1965, i.e., two years after the initial value of Eq. 6.9. The results are shown for the (relatively slow) HN profile, and one sees that the effects of both boundaries have traveled to the maximum in the mixing ratio. The faster DC profile gives a somewhat lower maximum mixing ratio, of the order of $20\text{-}25 \times 10^{-16}$, which is in better agreement with experiment. However, at this time the DC mixing ratio does not decrease above 30 km, which suggests that perhaps the high-altitude transport given by this model is too fast, and that the high-altitude value of the HN profile is more appropriate. The faster DC profile also leads to more rapid transport of the boundary conditions toward the maximum.

Figure 6-5 compares the observed global and Northern Hemisphere stratospheric burdens of ^{14}C with these computations (i.e., the initial condition of Eq. 6.9) for January 1963 with DC and HN K-profiles, and for the proper $^{14}CO_2$ boundary conditions as well as for the case of a perfect sink at both top (50 km) and bottom. One sees that, as would be expected, the effect of rapid transport with weak sinks tends to compensate for the case of slow transport with strong sinks. Note that the data provide a better fit to the global than to the Northern Hemispheric burden, the difference being transport to the Southern Hemisphere.

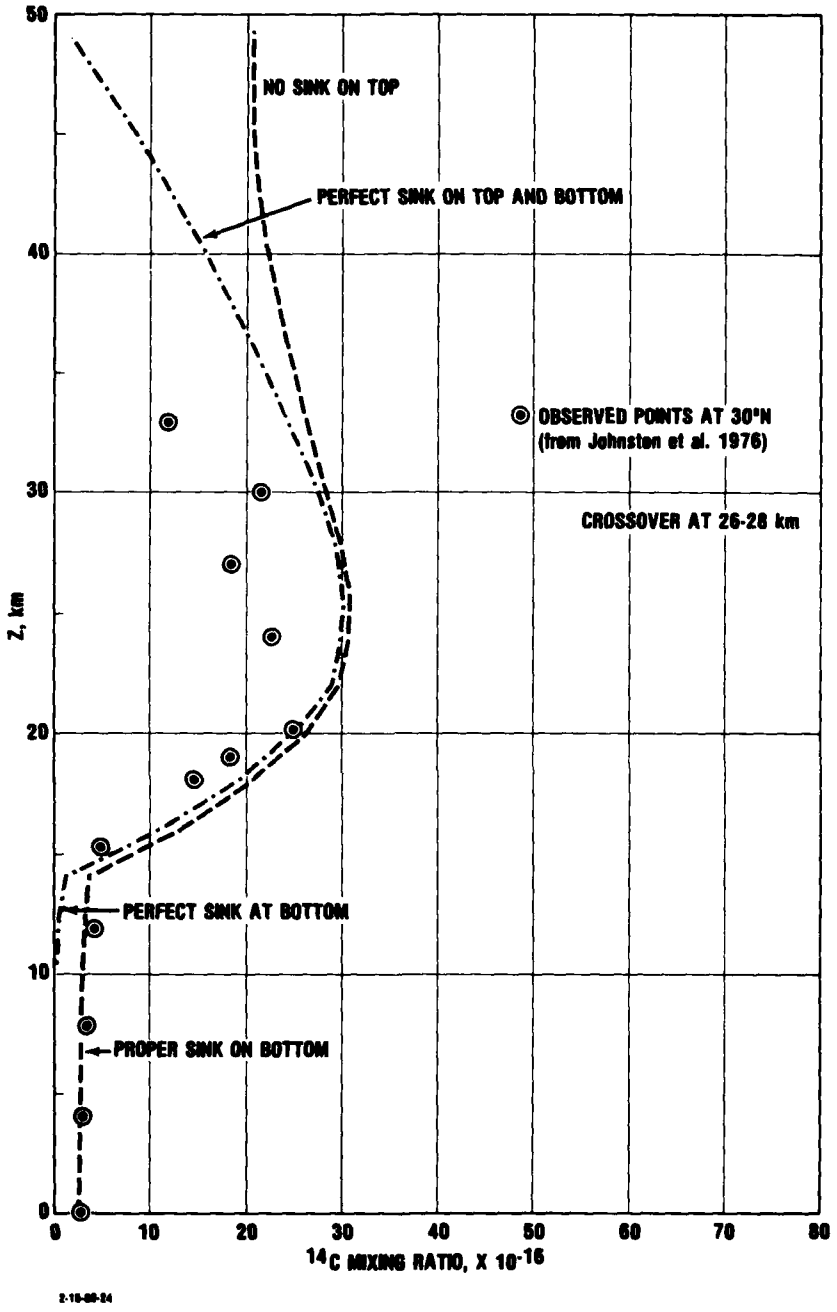

FIGURE 6-4. Profile of excess $^{14}CO_2$ two years after the initial value of Eq. 6.9, computed for the Hunten (HN) K-profile (Fig. 4-1). Note effects of varying boundary conditions (see discussion in Section 6.5).

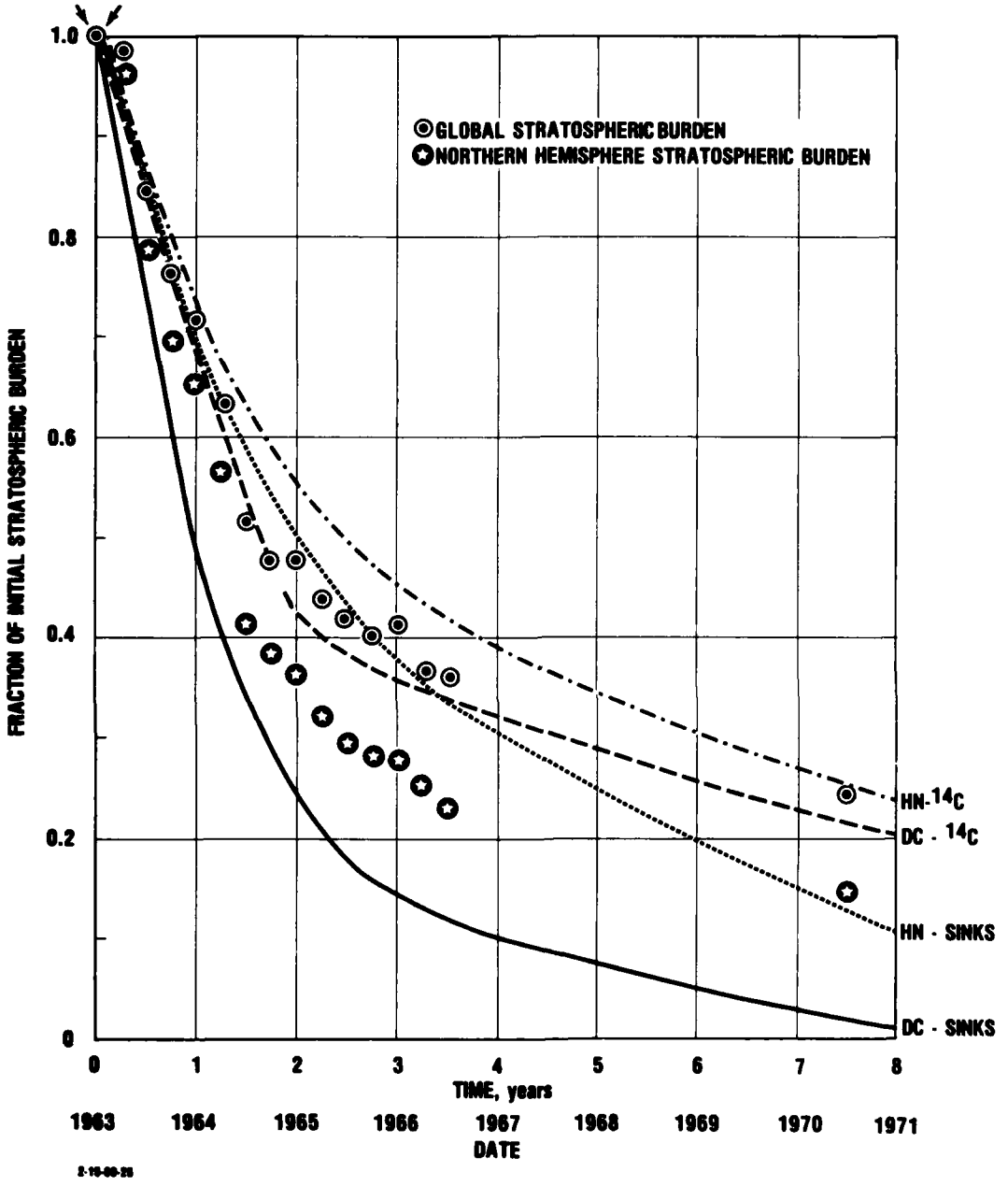

FIGURE 6-5. Decrease in burden of $^{14}CO_2$ following the initial value of Eq. 6.9. Note effects of varying K-profiles and boundary conditions in the modeling, and using global or Northern Hemisphere data (see discussion in Section 6.5). "Sinks" implies perfect sinks, f = 0, at both upper and lower boundaries.

In conclusion, the present calculation differs from the work of Johnston et al. (1976) in considering global stratospheric and tropospheric burdens rather than hemispheric altitude profiles, in emphasizing longer times after injection, and in a better treatment of the boundary conditions, so that the behavior of ^{90}Sr can be explained as well as that of $^{14}CO_2$.

7. CONCLUSIONS

The following conclusions may be drawn from the analysis of this paper:

1. The ^{95}Zr stratospheric data from six Chinese thermonuclear explosions demonstrate a strong seasonal variation in the decrease in stratospheric burden, with little stratosphere-to-troposphere transfer for a summer or fall injection until the next winter season. For a winter injection, rapid stratosphere-to-troposphere transfer starts immediately. (There have been no Chinese explosions in springtime.)

2. As far as decay in stratospheric burden is concerned, these data can be modeled in terms of one-dimensional (1-D) transport with a "fast" profile (such as DC or KD of Section 4, Fig. 4-1) for a winter injection. For a summer or fall injection it is again best to use a "fast" K-profile, but with the time of injection delayed until the next winter.

3. The ^{90}Sr and excess ^{14}C stratospheric burdens due to the USSR and U.S. nuclear tests of 1961-1962 have been analyzed with an extension of the same technique to take into account the variation in yield and latitude of the different bombs. The ^{90}Sr falls out much more rapidly than does the ^{14}C, principally because of the difference in lower boundary conditions. ^{90}Sr is rained out rapidly and completely, while ^{14}C (which is carried mainly as $^{14}CO_2$) is only absorbed slowly

(e-folding time of 4.5 years) by the ocean (and biosphere). Additional contributions to the difference come from the sedimentation of ^{90}Sr and from its lower effective injection height.

4. The falloff in stratospheric burden of ^{90}Sr, and of stratospheric and tropospheric burdens of ^{14}C, can be fitted well by using a "low" injection height ("Seitz" model of Section 3) and a "fast" K-profile (such as DC or KD of Section 4). Any other combination of injection height and K-profile gives significantly slower decay in burdens of these tracers than the observations show.

5. Reference to Fig. 2-7 shows that the inferred stratospheric burden of HTO falls off somewhat more slowly than that of ^{90}Sr and (especially at later times) significantly faster than that of $^{14}CO_2$. This can be explained as follows:

   a. T is a tracer of fusion rather than fission, so its effective injection height is somewhat larger than that of ^{14}C and definitely larger than that of ^{90}Sr.

   b. HTO is a gas, so it is not subject to sedimentation as ^{90}Sr is.

   c. HTO is precipitation scavenged in the troposphere and is lost on the ground after a large injection, so its lower boundary condition resembles that of ^{90}Sr rather than that of $^{14}CO_2$.

6. It is not necessary to postulate extra-rapid sedimentation of ^{90}Sr or a large unobserved high-altitude reservoir of ^{14}C to explain the difference in decay of these tracers.

7. The interpretation of Johnston et al. (1976) that the ^{14}C profile data require relatively slow (HN) transport is shown to be related both to their selection of relatively short sampling intervals and to their incorrect choice of boundary conditions.

BIBLIOGRAPHY

Bauer, E., "A Catalog of Perturbing Influences on Stratospheric Ozone, 1955-1975," Federal Aviation Administration Report No. FAA-EQ-78-20, (IDA Paper P-1340), September 1978.

Bauer, E., "The Computer Code DIFFUS," IDA memorandum for the record, February 1980.

Bauer, E. and K. A. Gardner, "Computations of Injection Coefficients and Residence Times for 1-D Models," Appendix D in Oliver et al., March 1977.

Bauer, E., R. C. Oliver, and W. Wasylkiwskyj, "On the Use of Zr-95 Data from Chinese Atmospheric Thermonuclear Explosions to Study Stratospheric Transport in a 1-D Parameterization," *J. Geophys. Res., 83,* 4019, 1978.

Chang, J. S., W. H. Duewer, and D. J. Wuebbles, "The Atmospheric Nuclear Tests of the 50's and 60's: A Possible Test of Ozone Depletion," *J. Geophys. Res.,* 1755, 1979.

Crutzen, P. J. and C. J. Howard, "The Effect of the HO_2 + NO Reaction Rate Constant on 1-D Model Calculations of Stratospheric Ozone Perturbations," *PAGEOPH, 116,* 497, 1978.

Danielsen, E. R., private communication, February 1979.

Donahue, T. M., "Hydrogen," in *The Upper Atmosphere and Magnetosphere,* National Academy of Sciences, 1977.

Ehhalt, D., "Turnover Times of Cs-137 and HTO in the Troposphere and Removal Rates of Natural Aerosol Particles and Water Vapor," *J. Geophys. Res., 78,* 7076, 1973.

Ellsaesser, H. W., "Model of the Stratospheric Water Budget and Its Validity," in CIAP Monograph 3, *The Stratosphere Perturbed by Propulsion Effluents,* DOT-TST-75-53, September 1975.

Ellsaesser, H. W., J. E. Harries, and D. Kley, *Stratospheric H_2O,* preprint UCRL-82542, Rev. 1, 1979.

Federal Radiation Council, *Estimates and Evaluation of Fallout in the U.S. from Nuclear Weapons Testing Conducted Through 1962*, Report No. 4, May 1963.

Feely, H. W., "Worldwide Deposition of ^{90}Sr Through 1975," Department of Energy Report HASL-308, p. I-121, October 1976.

Foley, H. M. and M. A. Ruderman, "Stratospheric NO Production from Past Nuclear Explosions, and Its Relevance to Projected SST Pollution," IDA Paper P-984, 1972. See also *J. Geophys. Res.*, *78*, 4441, 1973.

Friedman, I., L. Machta, and R. Soller, "Water Vapor Exchange Between a Water Droplet and Its Environment," *J. Geophys. Res.*, *67*, 2761, 1962.

Friend, J. P., H. W. Feely, P. W. Krey, J. Spar, and A. Walton, *The High-Altitude Sampling Program*, Isotopes, Inc., Report DASA 1300, August 1961.

Hamill, P., O. B. Toon, and C. S. Kiang, "Microphysical Processes Affecting Stratospheric Aerosol Particles," *J. Atmos. Sci.*, *34*, 1104, 1977.

Harley, N., I. Fisenne, L. D. Y. Ong, and J. Harley, "Fission Yield and Fission Product Decay," U. S. Department of Energy Report HASL-164, 251, 1965.

Harley, J. H., "A Brief History of Long-Range Fallout," Department of Energy Report HASL-306, P. I-3, July 1976.

HASL, "Final Tabulation of Monthly ^{90}Sr Fallout Data: 1945-1976," Department of Energy Report HASL-329, October 1977.

Hudson, R. D., Ed., "Chlorofluoromethanes and the Stratosphere," *NASA Reference Publication, 1010*, August 1977.

IAEA-International Atomic Energy Agency, "Environmental Isotope Data; World Survey of Isotope Concentration in Precipitation," No. 1, 1953-1963 (1969); No. 2, 1964-1965 (1970); No. 3, 1966-1967 (1971); No. 4, 1968-1969 (1973); No. 5, 1970-1971 (1975).

Jacobi, W. and K. Andre, "The Vertical Distribution of Ru-222, Ru-220, and Their Decay Products in the Atmosphere," *J. Geophys. Res.*, *68*, 3799, 1963.

Jacobs, D. G., "Sources of Tritium and Its Behavior Upon Release to the Atmosphere," AEC Critical Review Series TID-24635, 1968.

Johnston, H. S., D. Kattenhorn, and G. Whitten, "Use of Excess Carbon 14 Data to Calibrate Models of Stratospheric Ozone Depletion by Supersonic Transports," *J. Geophys. Res., 81,* 368, 1976.

Junge, C. E., C. W. Chagnon, and J. E. Manson, "Stratospheric Aerosols," *J. Meteor., 18,* 81, 1961.

Kasten, F., "Falling Speeds of Aerosol Particles," *J. Appl. Meteor., 7,* 944, 1968.

Krey, P. W. and B. Krajewski, "Tropospheric Scavenging of Sr-90 and T," in *Precipitation Scavenging,* AEC Symposium Series 22, 1970.

Krey, P. W., M. Schonberg, and L. Toonkel, "Updating Stratospheric Inventories to January 1973," U.S. Department of Energy Report HASL-281, 130, 1974.

Leifer, R. and L. Toonkel, "Updating Stratospheric Inventories to April 1977," Environmental Measurements Laboratory, Department of Energy, New York, Report EML-334, 1978.

Machta, L., "Prediction of CO_2 in the Atmosphere," *Carbon and the Biosphere,* G. M. Woodwell and E. V. Pecan, Eds., Department of Energy Symposium Series 30, Conf. 720510, August 1973.

Machta, L., "Status of Global Fallout Prediction," p. 369 in A. W. Klement, Jr., Ed., Radioactive Fallout from Nuclear Weapons Tests, DOE CONF-765, November 1965.

Machta, L., K. Telegadas, and R. J. List, "Meteorology of Fallout from 1961-1962 Nuclear Tests," Congress of the U.S.A., Hearing before Subcommittee on Research, Development and Radiation of the Joint Committee on Atomic Energy, 88th Congress, June 1963.

Mahlman, J. D., "Some Fundamental Limitations of Simplified Transport Models as Implied by Results from a Three-Dimensional General Circulation Tracer Model," p. 132 in Proc. Fourth Conference on CIAP, T. M. Hard and A. J. Broderick, Eds., U.S. Department of Transportation Report DOT-TSC-OST-75-38, August 1976.

Mason, A. S., "HT and HTO from Project Airstream, 1975-1977," University of Miami Tritium Laboratory Data Release #78-25, June 1978.

Mason, A. S. and H. G. Östlund, "Atmospheric HT and HTO, 3 Vertical Transport of Water in the Stratosphere," *J. Geophys. Res., 81,* 5349, 1976.

McCracken, D. D. and E. S. Dorn, *Numerical Methods and FORTRAN Programming*, J. Wiley, 1964.

Miskel, J. A., "Production of Tritium by Nuclear Weapons," in *Tritium*, A. A. Moghissi and M. W. Carter, Eds., Messenger Graphics, Phoenix, Arizona, 1973.

National Academy of Sciences, *Environmental Impact of Stratospheric Flight: Biological and Climatic Effects of Aircraft Emissions in the Stratosphere*, Washington, D.C., 1975.

NCRP-National Council on Radiation Protection and Measurements, "Tritium in the Environment," Report No. 62, March 1979.

Oliver, R. C., et al., "Recent Developments in the Estimation of Potential Effects of High Altitude Aircraft Emissions on Ozone and Climate," (IDA P-1343) FAA Report FAA-AEE-78-24, October 1978.

Oliver, R. C., et al., "Aircraft Emissions: Potential Effects on Ozone and Climate," (IDA P-1207) FAA Report FAA-EQ-77-3, March 1977.

Peterson, K. R., "An Empirical Model for Estimating World-Wide Deposition from Atmospheric Nuclear Detonation," *Health Physics*, *18*, 357-378, 1970.

Poppoff, I. G., R. C. Whitten, R. P. Turco, and L. A. Capone, "An Assessment of the Effect of Supersonic Aircraft Operations on the Stratospheric Ozone Content," NASA Reference Publication 1026, August 1978.

Richtmyer, R. D., and K. W. Morton, "Difference Methods for Initial-Value Problems," Second Edition, *Interscience*, 1967.

Salter, L. P., "Stratospheric Radioactivity in the Southern Hemisphere from 1961 and 1962 Weapons Tests," *Radioactive Fallout from Nuclear Weapons Tests*, A. W. Klement, Jr., Ed., Department of Energy Symposium Series 50, Conf. 765, November 1965.

Schell, W. R., G. Sauzay, and B. R. Payne, "World Distribution of Environmental Tritium," Proceedings of a Symposium, Vienna, November 1973 (IAEA-SM-181/34).

Schmeltekopf, A. J., et al., "Stratospheric Nitrous Oxide Altitude Profiles at Various Latitudes," *J. Atmos. Sci.*, *34*, 729, 1977.

Schwartz, S. E., "Residence Times in Reservoirs Under Non-Steady-State Conditions: Application to Atmospheric SO_2 and Aerosol Sulfate," *Tellus*, *31*, 530, 1979.

Singh, H. B., L. J. Salas, H. Shigeishi, and E. Scribner, "Atmospheric Halocarbons, Hydrocarbons, and Sulfur Hexafluoride: Global Distributions, Sources and Sinks," *Science*, *203*, 899, 1979.

Sowl, R. E., J. Gray, Jr., T. E. Ashenfelter, and K. Telegadas, "C-14 Measurements in the Stratosphere from a Balloon-Borne Molecule Sieve Sample," Department of Energy Report HASL-294, 20, 1975.

Sullivan, H. M. and D. M. Hunten, "Lithium, Sodium, and Potassium in the Twilight Airglow," *Can. J. Phys.*, *42*, 937, 1974.

Telegadas, K., "The Seasonal Stratospheric Distribution of Cd-109, Pu-238, and Sr-90," Department of Energy Report HASL-184, I-53, January 1968.

Telegadas, K., "The Seasonal Stratospheric Distribution and Circulation of Excess C-14 from March 1955 to July 1969," Department of Energy Report HASL-243, p. I-3, July 1971.

Telegadas, K., "Radioactivity Distribution in the Stratosphere from Chinese and French High-Yield Nuclear Tests (1967-1970)," Department of Energy Report HASL-281, p. I-3, April 1974.

Telegadas, K., "Radioactivity Distribution in the Stratosphere from the Chinese High-Yield Nuclear Test of June 27, 1973," Department of Energy Report HASL-298, N.Y., p. I-7, January 1976.

Telegadas, K., letter to A. S. Mason and E. Bauer, dated January 8, 1979 on Zr-95 and HTO data from Airstream missions, 1975-1977, 1979a.

Telegadas, K., "Estimation of Maximum Credible Atmospheric Radioactivity Concentrations and Dose Rates from Nuclear Tests," *Atmos. Environ.*, *13*, 327, 1979b.

Telegadas, K., "Radioactivity Distribution in the Stratosphere from the Chinese High-Yield Nuclear Test of November 17, 1976," Department of Energy Report EML-356, p. I-2, July 1979c.

Telegadas, K., letter to A. S. Mason and E. Bauer dated July 12, 1979 on HTO and Zr-95 data from 1978 Airstream missions, July 12, 1979d.

Toon, O. B., R. P. Turco, P. Hamill, C. S. Kiang, and R. C. Whitten, "A 1-D Model Describing Aerosol Formation and Evolution in the Stratosphere - II. Sensitivity Studies and Comparison with Observations," *J. Atmos. Sci.*, *36*, 718, 1979.

Turco, R. P., P. Hamill, O. B. Toon, R. C. Whitten, and C. S. Kiang, "A 1-D Model Describing Aerosol Formation and Evolution in the Stratosphere - I. Physical Processes and Numerical Analogs," *J. Atmos. Sci.*, *36*, 699, 1979.

Volchok, H. L., and M. T. Kleinman, "Global ^{90}Sr Fallout and Precipitation," Department of Energy Report HASL-245, p. I-2, October 1971.

*U.S. GOVERNMENT PRINTING OFFICE : 1980 0-721-895/289

END

DATE
FILMED

1-81

DTIC